Computer Science Technical Report
CSTR-3/2014
March 20, 2014

R. Ştefănescu, A. Sandu, I.M. Navon

"POD/DEIM Reduced-Order Strategies for Efficient Four Dimensional Variational Data Assimilation"

Computational Science Laboratory
Computer Science Department
Virginia Polytechnic Institute and State University
Blacksburg, VA 24060
Phone: (540)-231-2193
Fax: (540)-231-6075
Email: sandu@cs.vt.edu
Web: http://csl.cs.vt.edu

Innovative Computational Solutions

POD/DEIM Reduced-Order Strategies for Efficient Four Dimensional Variational Data Assimilation

Răzvan Ştefănescu [*1], Adrian Sandu [†1], and Ionel Michael Navon [‡2]

[1]Computational Science Laboratory, Department of Computer Science, Virginia Polytechnic Institute and State University, Blacksburg, Virginia, USA, 24060

[2]Department of Scientific Computing,The Florida State University, Tallahassee, Florida, USA, 32306

Abstract

This work studies reduced order modeling (ROM) approaches to speed up the solution of variational data assimilation problems with large scale nonlinear dynamical models. It is shown that a key ingredient for a successful reduced order solution to inverse problems is the consistency of the reduced order Karush-Kuhn-Tucker conditions with respect to the full optimality conditions. In particular, accurate reduced order approximations are needed for both the forward dynamical model and for the adjoint model. New bases selection strategies are developed for Proper Orthogonal Decomposition (POD) ROM data assimilation using both Galerkin and Petrov-Galerkin projections. For the first time POD, tensorial POD, and discrete empirical interpolation method (DEIM) are employed to develop reduced data assimilation systems for a geophysical flow model, namely, the two dimensional shallow water equations. Numerical experiments confirm the theoretical findings. In case of Petrov-Galerkin reduced data assimilation stabilization strategies must be considered for the reduced order models. The new hybrid tensorial POD/DEIM shallow water ROM data assimilation system provides analyses similar to those produced by the full resolution data assimilation system in one tenth of the computational time.

Keywords: inverse problems; proper orthogonal decomposition; discrete empirical interpolation method (DEIM); reduced-order models (ROMs); shallow water equations; finite difference methods;

[*]rstefane@vt.edu

[†]sandu@cs.vt.edu

[‡]inavon@fsu.edu

1 Introduction

Optimal control problems for nonlinear partial differential equations often require very large computational resources. Recently the reduced order approach applied to optimal control problems for partial differential equations has received increasing attention as a way of reducing the computational effort. The main idea is to project the dynamical system onto subspaces consisting of basis elements that represent the characteristics of the expected solution. These low order models serve as surrogates for the dynamical system in the optimization process and the resulting small optimization problems can be solved efficiently.

Application of Proper Orthogonal Decomposition (POD) to solve optimal control problems has proved to be successful (Kunisch and Volkwein [41], Kunisch et al. [45], Ito and Kunisch [35, 36], Kunisch and Xie [44]). However this approach may suffer from the fact that the basis elements are computed from a reference trajectory containing features which are quite different from those of the optimally controlled trajectory. A priori it is not evident what is the optimal strategy to generate snapshots for the reduced POD control procedure. A successful POD based reduced optimization should represent correctly the dynamics of the flow that is altered by the controller. To overcome the problem of unmodelled dynamics in the basis Afanasiev and Hinze [1], Ravindran [53], Kunisch and Volkwein [42] proposed to update the basis according to the current optimal control. In Arian et al. [6] this updating technique was combined with a trust region (TR) strategy to determine whether after an optimization step an update of the POD-basis should be performed. Additional work on TR/POD proved its efficiency, see Bergmann and Cordier [11], Leibfritz and Volkwein [47], Sachs and Volkwein [57]. Other studies proposed to include time derivatives, nonlinear terms, and adjoint information (see Diwoky and Volkwein [23], Hinze and Volkwein [31], Gubisch and Volkwein [29]) into POD basis for reduced order optimization purposes. A-posteriori analysis for POD applied to optimal control problems governed by parabolic and elliptic PDEs were developed in Hinze and Volkwein [31, 32], Tonna et al. [62], Tröltzsch and Volkwein [63], Kahlbacher and Volkwein [37], Kammann et al. [38]. Optimal snapshot location strategies for selecting additional snapshots at different time instances and for changing snapshots weights to represent more accurately the reduced order solutions were introduced in Kunisch and Volkwein [43]. Extension to parameterized nonlinear systems is available in Lass and Volkwein [46].

POD was successfully applied to solve strong constraint four dimensional variational (4D-Var) data assimilation problems for oceanic Cao et al. [13], Fang et al. [26] and atmospheric models Chen et al. [18, 17], Daescu and Navon [19, 20], Du et al. [24]. A strategy that formulates first order optimality conditions starting from POD models has been implemented in 4D-Var systems in Vermeulen and Heemink [64], Sava [58], while hybrid methods using reduced adjoint models but optimizing in full space were introduced in Altaf et al. [2], Ambrozic [3]. POD/DEIM has been employed to reduce the CPU complexity of a 1D Burgers 4D-Var system in Baumann [10]. Recently Amsallem et al. [5] used a two-step gappy POD procedure to decrease the computational com-

plexity of the reduced nonlinear terms in the solution of shape optimization problems. Reduced basis approximation (Barrault et al. [8], Grepl and Patera [28], Patera and Rozza [51], Rozza et al. [54], Dihlmann and Haasdonk [21]) is known to be very efficient for parameterized problems and recently has been applied in the context of reduced order optimization by Gubisch and Volkwein [29].

This paper develops a systematic approach to POD bases selection for Petrov-Galerkin based reduced order data assimilation systems with non-linear models. The fundamental idea is to provide an order reduction strategy that ensures the consistency of reduced Karush Kuhn Tucker (KKT) optimality conditions with the full KKT optimality conditions. This research extends the results of Hinze and Volkwein [32] by considering nonlinear models and Petrov-Galerkin projections. Moreover, the POD basis construction strategies proposed here can be used for every type of reduced optimization involving adjoint models and projection based reduced order methods including reduced basis approach.

The proposed reduced order strategy is applied to solve a 4D-Var data assimilation problem with the two dimensional shallow water equations model. We compare three reduced 4D-Var data assimilation systems using three different POD based reduced order methods namely standard POD, tensorial POD and standard POD/DEIM (see Stefanescu et al. [61]). To the best of our knowledge this is the first application of POD/DEIM to obtain suboptimal solutions of reduced data assimilation system governed by a geophysical 2D flow model. For the mesh size used in our experiments the hybrid POD/DEIM reduced data assimilation system is approximately 10 times faster then the full space data assimilation system, and this ratio is found out to be directly proportional with the the mesh size.

The remainder of the paper is organized as follows. Section 2 introduces the optimality condition for the standard 4D-Var data assimilation problem. Section 3 reviews the reduced order modeling methodologies deployed in this work: standard, tensorial, and DEIM POD. Section 4 describes the theoretical path that leads to efficient POD bases selection strategies for reduced POD 4D-Var data assimilation systems governed by nonlinear state models using both Petrov-Galerkin and Galerkin projections. Section 5 discusses the swallow water equations model and the three reduced order 4D-Var data assimilation systems employed for comparisons in this study. Results of extensive numerical experiments are discussed in Section 6 while conclusions are drawn in Section 7. An appendix describing the high-fidelity alternating direction fully implicit (ADI) forward, tangent linear and adjoint SWE discrete models is available.

2 Strong constraint 4D-Var data assimilation system

Variational data assimilation seeks the optimal parameter values that provide the best fit (in some well defined sense) of model outputs with physical observations. In this presentation we focus on the traditional approach where the model parameters are the initial conditions $\mathbf{x}_0$, however the discussion can be easily generalized to further include other model parameter as control variables.

In 4D-Var the following objective function that quantifies the model-data misfit and accounts for prior information is minimized:

$$\mathcal{J}(\mathbf{x}_0) = \frac{1}{2}\big(\mathbf{x}_0^{\mathrm{b}} - \mathbf{x}_0\big)^T \mathbf{B}_0^{-1}\big(\mathbf{x}_0^{\mathrm{b}} - \mathbf{x}_0\big) + \frac{1}{2}\sum_{i=0}^{N}\big(\mathbf{y}_i - \mathcal{H}\left(\mathbf{x}_i\right)\big)^T \mathbf{R}_i^{-1}\big(\mathbf{y}_i - \mathcal{H}\left(\mathbf{x}_i\right)\big), \quad \text{(1a)}$$

subject to the constraints posed by the nonlinear forward model dynamics

$$\mathbf{x}_{i+1} = \mathcal{M}_{i,i+1}\left(\mathbf{x}_i\right), \quad i = 0, .., N-1. \quad \text{(1b)}$$

Here $\mathbf{x}_0^{\mathrm{b}}$ is the background state and $\mathbf{x}_i$ are the state variables at observations time t_i, $i = 0, .., N$. The nonlinear state model $\mathcal{M}_{i,i+1}$, $i = 0, .., N-1$ advances the state variables in time. The background error covariance matrix is $\mathbf{B}_0$, the data $\mathbf{y}_i$ are the measurement (observation) values at times t_i, $i = 0, .., N$, and $\mathbf{R}_i$ represent the corresponding observation error covariance matrices. The nonlinear observation operator $\mathcal{H}$ maps the model state space to the observation space.

Using the Lagrange multiplier technique the constrained optimization problem (1) is replaced with the unconstrained optimization of the following Lagrangian function:

$$\begin{aligned}\mathcal{L}(\mathbf{x}_0) = \frac{1}{2}\big(\mathbf{x}_0^{\mathrm{b}} - \mathbf{x}_0\big)^T \mathbf{B}_0^{-1}\big(\mathbf{x}_0^{\mathrm{b}} - \mathbf{x}_0\big) + \frac{1}{2}\sum_{i=0}^{N}\big(\mathbf{y}_i - \mathcal{H}(\mathbf{x}_i)\big)^T \mathbf{R}_i^{-1}\big(\mathbf{y}_i - \mathcal{H}(\mathbf{x}_i)\big) + \\ \sum_{i=0}^{N-1}\lambda_{i+1}^T\big(\mathbf{x}_{i+1} - \mathcal{M}_{i,i+1}\left(\mathbf{x}_i\right)\big),\end{aligned} \quad \text{(2)}$$

where λ_i is the Lagrange multipliers vector at observation time t_i.

Next we derive the first order optimality conditions. The infinitesimal change in $\mathcal{L}$ due to the infinitesimal change $\delta\mathbf{x}_0$ in $\mathbf{x}_0$ is

$$\begin{aligned}\delta\mathcal{L}(\mathbf{x}_0) = -\delta\mathbf{x}_0^T \mathbf{B}_0^{-1}\big(\mathbf{x}_0^{\mathrm{b}} - \mathbf{x}_0\big) - \sum_{i=0}^{N}\delta\mathbf{x}_i^T \mathbf{H}_i^T \mathbf{R}_i^{-1}\big(\mathbf{y}_i - \mathcal{H}(\mathbf{x}_i)\big) + \\ \sum_{i=0}^{N-1}\lambda_{i+1}^T\big(\delta\mathbf{x}_{i+1} - \mathbf{M}_{i,i+1}\delta\mathbf{x}_i\big) + \sum_{i=0}^{N-1}\delta\lambda_{i+1}^T\big(\mathbf{x}_{i+1} - \mathcal{M}_{i,i+1}\left(\mathbf{x}_i\right)\big),\end{aligned} \quad \text{(3)}$$

where $\mathbf{H}_i$ and $\mathbf{M}_{i,i+1}$ are the linearized versions of $\mathcal{H}$ and $\mathcal{M}_{i,i+1}$ for all time instances t_i, $i = 0, \ldots, N-1$. The corresponding adjoint operators are $\mathbf{H}_i^T$ and $\mathbf{M}_{i+1,i}^*$, respectively. After rearranging the above equation and using again the definition of adjoint operators we obtain

$$\begin{aligned}\delta\mathcal{L}(\mathbf{x}_0) = -\delta\mathbf{x}_0^T \mathbf{B}_0^{-1}\big(\mathbf{x}_0^{\mathrm{b}} - \mathbf{x}_0\big) + \sum_{i=1}^{N-1}\delta\mathbf{x}_i^T\Big(\lambda_i - \mathbf{M}_{i+1,i}^*\lambda_{i+1} - \mathbf{H}_i^T\mathbf{R}_i^{-1}\big(\mathbf{y}_i - \mathcal{H}(\mathbf{x}_i)\big)\Big) + \\ \delta\mathbf{x}_N^T\Big(\lambda_N - \mathbf{H}_N^T\mathbf{R}_N^{-1}\big(\mathbf{y}_N - \mathcal{H}(\mathbf{x}_N)\big)\Big) - \delta\mathbf{x}_0^T\Big(\mathbf{H}_0^T\mathbf{R}_0^{-1}\big(\mathbf{y}_0 - \mathcal{H}(\mathbf{x}_0)\big) + \mathbf{M}_{1,0}^*\lambda_1\Big) + \\ \sum_{i=0}^{N-1}\delta\lambda_{i+1}^T\big(\mathbf{x}_{i+1} - \mathcal{M}_{i,i+1}\left(\mathbf{x}_i\right)\big).\end{aligned} \quad \text{(4)}$$

The first order necessary optimality conditions for the full-order 4D-Var are:

$$\textit{Forward model: } \mathbf{x}_{i+1} = \mathcal{M}_{i,i+1}\left(\mathbf{x}_i\right), \quad i = 0, .., N-1, \tag{5a}$$

$$\begin{aligned} \textit{Adjoint model: } \lambda_N &= \mathbf{H}_N^T \mathbf{R}_N^{-1}\big(\mathbf{y}_N - \mathcal{H}(\mathbf{x}_N)\big), \\ \lambda_i &= \mathbf{M}_{i+1,i}^* \lambda_{i+1} + \mathbf{H}_i^T \mathbf{R}_i^{-1}\big(\mathbf{y}_i - \mathcal{H}(\mathbf{x}_i)\big), \quad i = N-1, .., 0, \end{aligned} \tag{5b}$$

$$\textit{Cost function gradient: } \nabla_{\mathbf{x}_0}\mathcal{L} = -\mathbf{B}_0^{-1}\big(\mathbf{x}_0^{\mathrm{b}} - \mathbf{x}_0\big) - \lambda_0 = 0. \tag{5c}$$

3 Reduced order forward modeling

The most prevalent basis selection method for model reduction of nonlinear problems is the proper orthogonal decomposition, also known as Karhunen-Loève expansions (Karhunen [39], Loève [48]), principal component analysis (Hotelling [34]) , and empirical orthogonal functions (Lorenz [49]).

Three reduced order models will be considered in this paper: standard POD (SPOD), tensorial POD (TPOD), and standard POD/Discrete Empirical Interpolation Method (POD/DEIM), which were described in Stefanescu et al. [61] and Stefanescu and Navon [60]. The reduced Jacobians required by the ADI schemes are obtained analytically for all three ROMs and their computational complexity depends only on k the dimension of POD basis. The methods differ in the way the nonlinear terms are treated. We illustrate the application of the methods to reducing a polynomial quadratic nonlinearity $N(\mathbf{x}) = \mathbf{x}^2$. Details regarding standard POD approach including the snapshot procedure, POD basis computation and the corresponding reduced equations can be found in [61]. We assume a Petrov-Galerkin projection for constructing the reduced order models with the two biorthogonal projection matrices $U, W \in \mathbb{R}^{n\times k}$, $W^T U = I_k$, where I_k is the identity matrix of order k. U denotes the POD basis and the test functions are stored in W. We assume a POD expansion of the state $\mathbf{x} \approx U\tilde{\mathbf{x}}$, and obtain the reduced order quadratic term $\widetilde{N}(\tilde{\mathbf{x}}) \approx N(\mathbf{x})$.

Standard POD

$$\widetilde{N}(\tilde{\mathbf{x}}) = \underbrace{W^T}_{k\times n}\underbrace{\left(U\tilde{\mathbf{x}}\right)^2}_{n\times 1}, \quad \widetilde{N}(\tilde{\mathbf{x}}) \in \mathbb{R}^k, \tag{6}$$

where vector powers are taken component-wise and n is the number of spatial mesh points.

Tensorial POD

$$\widetilde{N}(\tilde{\mathbf{x}}) = \left[\widetilde{N}_i\right]_{i=1,..,k} \in \mathbb{R}^k; \quad \widetilde{N}_i = \sum_{j=1}^{k}\sum_{l=1}^{k} T_{i,j,l}\tilde{x}_j\tilde{x}_l, \tag{7}$$

where the rank-three tensor T is defined as

$$T = \left(T_{i,j,l}\right)_{i,j,l=1,..,k} \in \mathbb{R}^{k\times k\times k}, \quad T_{i,j,l} = \sum_{r=1}^{n} W_{i,r}U_{j,r}U_{l,r}.$$

Standard POD/DEIM

$$\tilde{N}(\tilde{\mathbf{x}}) \approx \underbrace{W^T V (P^T V)^{-1}}_{k\times m} \underbrace{\left(P^T U \tilde{\mathbf{x}}\right)^2}_{m\times 1}, \tag{8}$$

where m is the number of interpolation points, $V \in \mathbb{R}^{n\times m}$ gathers the first m POD basis modes of the nonlinear term while $P \in \mathbb{R}^{n\times m}$ is the DEIM interpolation selection matrix (Chaturantabut [14], Chaturantabut and Sorensen [15, 16]).

The systematic application of these techniques in the Petrov-Galerkin projection framework to (1b) leads to the following reduced order forward model

$$\tilde{\mathbf{x}}_{i+1} = \widetilde{\mathcal{M}}_{i,i+1}\left(\tilde{\mathbf{x}}_i\right), \quad \widetilde{\mathcal{M}}_{i,i+1}\left(\tilde{\mathbf{x}}_i\right) = W^T \mathcal{M}_{i,i+1}\left(U\tilde{\mathbf{x}}_i\right), \quad i = 0, .., N-1. \tag{9}$$

4 Reduced order 4D-Var data assimilation

Two major strategies for solving optimization problems with reduced order models have been discussed in the literature. The "reduced adjoint" (RA) approach projects the first order optimality equations (5a), (5b) and (5c) of the full system onto the POD reduced spaces, while the "adjoint of reduced" (AR) approach formulates the first order optimality conditions from the forward reduced order model (10b). Reduced order formulation of the cost function is employed in both cases (Dimitriu et al. [22], Vermeulen and Heemink [64]).

The "reduced of adjoint" approach constructs accurate low-order forward and adjoint models using separate bases; however it can represent poorly the gradient of the full cost function (2) since its not clear what information should be included in the reduced space where the gradient equation (5c) is projected.

A major concern with the "adjoint of reduced" approach is the lack of consistency in the optimality conditions with respect to the full system. The reduced forward model is accurate, but its adjoint approximates poorly the full adjoint system since the POD bases rely only on forward dynamics information. Consequently both the RA and the AR methods may lead to inaccurate suboptimal solutions.

The "adjoint of reduced" approach has been recently applied by Vermeulen and Heemink [64], Pelc et al. [52] to solve 4D-Var data assimilation problems. Snapshots from both primal and dual systems have been used for balanced truncation of a linear state-system [65]. Hinze and Volkwein [33] developed a-priori error estimates for linear quadratic optimal control problems using proper orthogonal decomposition. They state that error estimates for the adjoint state yield error estimates of the control suggesting that accurate reduced adjoint models with respect to the full adjoint model lead to more accurate suboptimal surrogate solutions. Numerical results confirmed that a POD manifold built on snapshots taken from both forward and adjoint trajectories provides more accurate reduced optimization systems.

Here we propose a systematic approach to select POD bases for reduced order data assimilation with non-linear models. The idea is to have a reduced KKT optimality

conditions that include an accurate reduced POD adjoint model with respect to the full adjoint model outputs. This new strategy combines the most desirable characteristics of both AR and RA approaches and provides a standard approach for general reduced order optimization problems.

4.1 Reduced order cost function

We first define the cost function for ROM data assimilation. To this end we assume that the forward POD manifold $U_{\rm f}$ is computed using only snapshots of the full forward model solution (the subscript denotes that only forward dynamics information is used for POD basis construction). The Petrov-Galerkin (PG) test functions $W_{\rm f}$ may be different than the trial functions $U_{\rm f}$. Assuming a POD expansion of $\mathbf{x} \approx U_{\rm f}\tilde{\mathbf{x}}$ the reduced data assimilation problem minimizes the following reduced order cost function

$$\begin{aligned}\mathcal{J}^{\rm POD}(\tilde{\mathbf{x}}_0) = &\frac{1}{2}\big(\mathbf{x}_0^{\rm b} - U_{\rm f}\tilde{\mathbf{x}}_0\big)^T\mathbf{B}_0^{-1}\big(\mathbf{x}_0^{\rm b} - U_{\rm f}\tilde{\mathbf{x}}_0\big) \\ &+ \frac{1}{2}\sum_{i=0}^{N}\big(\mathbf{y}_i - \mathcal{H}(U_{\rm f}\tilde{\mathbf{x}}_i)\big)^T\mathbf{R}_i^{-1}\big(\mathbf{y}_i - \mathcal{H}(U_{\rm f}\tilde{\mathbf{x}}_i)\big)^T,\end{aligned} \tag{10a}$$

subject to the constraints posed by the ROM projected nonlinear forward model dynamics

$$\tilde{\mathbf{x}}_{i+1} = \widetilde{\mathcal{M}}_{i,i+1}\left(\tilde{\mathbf{x}}_i\right), \quad \widetilde{\mathcal{M}}_{i,i+1}\left(\tilde{\mathbf{x}}_i\right) = W_{\rm f}^T\mathcal{M}_{i,i+1}\left(U_{\rm f}\tilde{\mathbf{x}}_i\right), \quad i = 0,..,N-1. \tag{10b}$$

An observation operator that maps directly from the reduced model space to observations space may be introduced. For clarity sake we will continue to use operator notation $\mathcal{H}$. $\widetilde{\mathcal{M}}_{i,i+1}$ is the PG reduced order forward model that propagates the reduced order state from t_i to t_{i+1} for $i = 0,..,N-1$.

4.2 The "adjoint of reduced forward model" approach

In the AR approach the constrained optimization problem (10) is replaced by an unconstrained one for the following reduced Lagrangian function

$$\begin{aligned}\mathcal{L}^{\rm POD}(\tilde{\mathbf{x}}_0) = &\frac{1}{2}\big(\mathbf{x}_0^{\rm b} - U_{\rm f}\tilde{\mathbf{x}}_0\big)^T\mathbf{B}_0^{-1}\big(\mathbf{x}_0^{\rm b} - U_{\rm f}\tilde{\mathbf{x}}_0\big) \\ &+ \frac{1}{2}\sum_{i=0}^{N}\big(\mathbf{y}_i - \mathcal{H}(U_{\rm f}\tilde{\mathbf{x}}_i)\big)^T\mathbf{R}_i^{-1}\big(\mathbf{y}_i - \mathcal{H}(U_{\rm f}\tilde{\mathbf{x}}_i)\big) + \sum_{i=0}^{N-1}\tilde{\lambda}_{i+1}^T\big(\tilde{\mathbf{x}}_{i+1} - \widetilde{\mathcal{M}}_{i,i+1}\left(\tilde{\mathbf{x}}_i\right)\big).\end{aligned} \tag{11}$$

The variation of $\mathcal{L}^{\text{POD}}$ is given by

$$\begin{aligned}\delta\mathcal{L}^{\text{POD}}(\tilde{\mathbf{x}}_0) = &-\delta\tilde{\mathbf{x}}_0^T\mathbf{B}_0^{-1}\big(\mathbf{x}_0^{\text{b}} - U_{\text{f}}\tilde{\mathbf{x}}_0\big) + \sum_{i=1}^{N-1}\delta\tilde{\mathbf{x}}_i^T\Bigg(\tilde{\lambda}_i - \widetilde{\mathbf{M}}_{i+1,i}^*\tilde{\lambda}_{i+1}\\ &- U_{\text{f}}^T\mathbf{H}_i^T\mathbf{R}_i^{-1}\big(\mathbf{y}_i - \mathcal{H}(U_{\text{f}}\tilde{\mathbf{x}}_i)\big)\Bigg) + \delta\tilde{\mathbf{x}}_N^T\Bigg(\tilde{\lambda}_N - U_{\text{f}}^T\mathbf{H}_N^T\mathbf{R}_N^{-1}\big(\mathbf{y}_N - \mathcal{H}(U_{\text{f}}\tilde{\mathbf{x}}_N)\big)\Bigg)\\ &- \delta\tilde{\mathbf{x}}_0^T\Bigg(U_{\text{f}}^T\mathbf{H}_0^T\mathbf{R}_0^{-1}\big(\mathbf{y}_0 - \mathcal{H}(U_{\text{f}}\tilde{\mathbf{x}}_0)\big) + \widetilde{\mathbf{M}}_{1,0}^*\tilde{\lambda}_1\Bigg) + \sum_{i=0}^{N-1}\delta\tilde{\lambda}_{i+1}^T\big(\tilde{\mathbf{x}}_{i+1} - \widetilde{\mathcal{M}}_{i,i+1}\left(\tilde{\mathbf{x}}_i\right)\big),\end{aligned} \tag{12}$$

where

$$\widetilde{\mathbf{M}}_{i+1,i}^* = U_{\text{f}}^T\mathbf{M}_{i,i+1}^T W_{\text{f}}, \quad i = 0, .., N-1$$

is the adjoint of the reduced order linearized forward model $\mathcal{M}_{i,i+1}$. The AR reduced KKT conditions are:

AR reduced forward model: (13a)

$$\tilde{\mathbf{x}}_{i+1} = \widetilde{\mathcal{M}}_{i,i+1}\left(\tilde{\mathbf{x}}_i\right), \quad i = 0, .., N-1,$$

AR reduced adjoint model: (13b)

$$\begin{aligned}&\tilde{\lambda}_N = U_{\text{f}}^T\mathbf{H}_N^T R_N^{-1}\big(\mathbf{y}_N - H(U_{\text{f}}\tilde{\mathbf{x}}_N)\big),\\ &\tilde{\lambda}_i = U_{\text{f}}^T\mathbf{M}_{i,i+1}^T W_{\text{f}}\tilde{\lambda}_{i+1} + U_{\text{f}}^T\mathbf{H}_i^T\mathbf{R}_i^{-1}\big(\mathbf{y}_i - \mathcal{H}(U_{\text{f}}\tilde{\mathbf{x}}_i)\big), \quad i = N-1, .., 0,\end{aligned}$$

AR cost function gradient : (13c)

$$\nabla_{\tilde{\mathbf{x}}_0} J^{POD} = -U_{\text{f}}^T\mathbf{B}_0^{-1}\big(\mathbf{x}_0^{\text{b}} - U_{\text{f}}\tilde{\mathbf{x}}_0\big) - \tilde{\lambda}_0 = 0.$$

4.3 The "reduced order adjoint model" approach

In the RA approach the full forward (5a) and full adjoint (5b) models are projected onto separate reduced manifolds. Let U_{f} and U_{a} be the POD bases obtained from snapshots of the full forward and adjoint model solutions, respectively. The ROM approximation of the full forward state is $\mathbf{x}_i \approx U_{\text{f}}\tilde{\mathbf{x}}_i$, and of the full adjoint state is $\lambda_i \approx U_{\text{a}}\tilde{\lambda}_i$, $i = 0, .., N$. The test functions for the forward and adjoint models are W_{f} and W_{a} respectively. The reduced order forward and adjoint models are

RA reduced forward model: (14a)

$$\tilde{\mathbf{x}}_{i+1} = \widetilde{\mathcal{M}}_{i,i+1}\left(\tilde{\mathbf{x}}_i\right), \quad \widetilde{\mathcal{M}}_{i,i+1}\left(\tilde{\mathbf{x}}_i\right) = W_{\text{f}}^T\mathcal{M}_{i,i+1}\left(U_{\text{f}}\tilde{\mathbf{x}}_i\right), \quad i = 0, .., N-1,$$

RA reduced adjoint model: (14b)

$$\begin{aligned}&\tilde{\lambda}_N = W_a^T\mathbf{H}_N^T\mathbf{R}_N^{-1}\big(\mathbf{y}_N - H(U_{\text{f}}\tilde{\mathbf{x}}_N)\big),\\ &\tilde{\lambda}_i = W_{\text{a}}^T\mathbf{M}_{i,i+1}^T U_{\text{a}}\tilde{\lambda}_{\mathbf{i+1}} + W_{\text{a}}^T\mathbf{H}_i^T\mathbf{R}_i^{-1}\big(\mathbf{y}_i - \mathcal{H}(U_{\text{f}}\tilde{\mathbf{x}}_i)\big), \quad i = N-1, .., 0.\end{aligned}$$

Clearly this approach will ensure accurate low-order forward and adjoint models. However, the question that remains is how to construct a reduced order basis for the gradient equation (5c).

4.4 The ARRA approach: ensuring consistency of the first order optimality system

We provide the answer by requiring that the AR reduced adjoint model (13b) coincides with the RA reduced adjoint model(14b). This is achieved by choosing

$$W_{\mathrm{f}} = U_{\mathrm{a}} \text{ and } W_{\mathrm{a}} = U_{\mathrm{f}}. \tag{15}$$

This approach provides a consistent reduced order KKT system, in the sense that the AR reduced adjoint model (13b) is an accurate approximation of the full adjoint model.

By selecting POD bases in this manner the reduced gradient (13c) accurately approximates the full gradient (5c) in the reduced POD subspace U_{f} since $\tilde{\lambda}_0 = W_a^T \lambda_0 = U_{\mathrm{f}}^T \lambda_0$ and

$$\nabla_{\tilde{\mathbf{x}}_0} J^{POD} = U_{\mathrm{f}}^T \left(-\mathbf{B}_0^{-1} \left(\mathbf{x}_0^{\mathrm{b}} - U_{\mathrm{f}} \tilde{\mathbf{x}}_0 \right) - \lambda_0 \right) = 0. \tag{16}$$

We refer to this techniques coincide as "adjoint of reduced + reduced of adjoint" (ARRA). It improves the AR approach since each of the first two reduced optimality conditions (13) is a surrogate model that accurately represents the corresponding full order model. In the traditional RA case the full gradient equation (5c) is projected either onto the trial POD basis of the forward model or on the test functions POD basis of the adjoint model. In the ARRA approach the reduced order optimality condition (16) is the projection of the full order optimality condition (5c).

The Petrov-Galerkin projection does not guarantee the stability of the ARRA reduced order forward model (14a)–(15). In our numerical experiments this approach exhibited large instabilities when the initial conditions were slightly perturbed from the ones used to generate POD manifolds. Stabilization approaches as the ones discussed by Amsallem and Farhat [4] and Bui-Thanh et al. [12] can be employed and are the subject of on-going research.

In this paper we focus on Galerkin POD reduced models that preserve the stability of the full forward model. In the Galerkin approach we have $W_{\mathrm{f}} = U_{\mathrm{f}}$ and $W_{\mathrm{a}} = U_{\mathrm{a}}$, and from (15) we obtain $U_{\mathrm{f}} = U_{\mathrm{a}}$. The POD basis must coincide for both forward and adjoint reduced models. This unique basis has to represent accurately both the full forward and the full adjoint models. Therefore we propose to take the union of snapshots of the full forward solutions and snapshots of the full adjoint solutions. The POD basis is constructed from the dominant eigenvectors of the correlation matrix of the aggregated snapshots of full forward and adjoint model outputs.

5 4D-Var data assimilation with the shallow water equations

5.1 SWE model

SWE has proved its capabilities in modeling propagation of Rossby and Kelvin waves in the atmosphere, rivers, lakes and oceans as well as gravity waves in a smaller domain. The alternating direction fully implicit finite difference scheme Gustafsson [30]

was considered in this paper and it is stable for large CFL condition numbers (we tested the stability of the scheme for a CFL condition number equal up to 8.9301). We refer to Fairweather and Navon [25], Navon and Villiers [50] for other research work on this topic.

The SWE model using the β-plane approximation on a rectangular domain is introduced (see Gustafsson [30])

$$\frac{\partial w}{\partial t} = A(w)\frac{\partial w}{\partial x} + B(w)\frac{\partial w}{\partial y} + C(y)w, \quad (x,y) \in [0,L] \times [0,D], \quad t \in (0, t_{\mathrm{f}}], \tag{17}$$

where $w = (u, v, \phi)^T$ is a vector function, u, v are the velocity components in the x and y directions, respectively, h is the depth of the fluid, g is the acceleration due to gravity, and $\phi = 2\sqrt{gh}$.

The matrices A, B and C are assuming the form

$$A = -\begin{pmatrix} u & 0 & \phi/2 \\ 0 & u & 0 \\ \phi/2 & 0 & u \end{pmatrix}, \quad B = -\begin{pmatrix} v & 0 & 0 \\ 0 & v & \phi/2 \\ 0 & \phi/2 & v \end{pmatrix}, \quad C = \begin{pmatrix} 0 & f & 0 \\ -f & 0 & 0 \\ 0 & 0 & 0 \end{pmatrix},$$

where f is the Coriolis term

$$f = \hat{f} + \beta(y - D/2), \quad \beta = \frac{\partial f}{\partial y}, \quad \forall\, y,$$

with $\hat{f}$ and β constants.

We assume periodic solutions in the x direction for all three state variables while in the y direction

$$v(x, 0, t) = v(x, D, t) = 0, \quad x \in [0, L], \quad t \in (0, t_{\mathrm{f}}]$$

and Neumann boundary condition are considered for u and ϕ.

Initially $w(x, y, 0) = \psi(x, y), \quad \psi : \mathbb{R} \times \mathbb{R} \to \mathbb{R}, \quad (x, y) \in [0, L] \times [0, D]$. Now we introduce a mesh of $n = N_x \cdot N_y$ equidistant grid points on $[0, L] \times [0, D]$, with $\Delta x = L/(N_x - 1), \quad \Delta y = D/(N_y - 1)$. We also discretize the time interval $[0, t_{\mathrm{f}}]$ using N_t equally distributed points and $\Delta t = t_{\mathrm{f}}/(N_t - 1)$. Next we define vectors of unknown variables of dimension n containing approximate solutions such as

$$\boldsymbol{w}(t_N) \approx [w(x_i, y_j, t_N)]_{i=1,2,..,N_x, \quad j=1,2,..,N_y} \in \mathbb{R}^n, \quad N = 1, 2, ..N_t.$$

The semi-discrete equations of SWE (17) are:

$$\mathbf{u}' = -F_{11}(\mathbf{u}) - F_{12}(\boldsymbol{\phi}) - F_{13}(\mathbf{u}, \mathbf{v}) + \mathbf{F} \odot \mathbf{v}, \tag{18}$$

$$\mathbf{v}' = -F_{21}(\mathbf{u}) - F_{22}(\mathbf{v}) - F_{23}(\boldsymbol{\phi}) - \mathbf{F} \odot \mathbf{u}, \tag{19}$$

$$\boldsymbol{\phi}' = -F_{31}(\mathbf{u}, \boldsymbol{\phi}) - F_{32}(\mathbf{u}, \boldsymbol{\phi}) - F_{33}(\mathbf{v}, \boldsymbol{\phi}) - F_{34}(\mathbf{v}, \boldsymbol{\phi}), \tag{20}$$

where $\mathbf{u}'$, $\mathbf{v}'$, $\boldsymbol{\phi}'$ denote semi-discrete time derivatives, $\mathbf{F} \in \mathbb{R}^n$ stores Coriolis components while the nonlinear terms $F_{i,j}$ are defined as follows:

$$
\begin{aligned}
&F_{11}, F_{12}, F_{21}, F_{23} : \mathbb{R}^n \to \mathbb{R}^n, \quad F_{13}, F_{22}, F_{3i} : \mathbb{R}^n \times \mathbb{R}^n \to \mathbb{R}^n, \quad i = 1, 2, 3, 4, \\
&\quad F_{11}(\mathbf{u}) = \boldsymbol{u} \odot A_x \boldsymbol{u}, \quad F_{12}(\boldsymbol{\phi}) = \frac{1}{2}\boldsymbol{\phi} \odot A_x \boldsymbol{\phi}, \quad F_{13}(\boldsymbol{u}, \boldsymbol{v}) = \boldsymbol{v} \odot A_y \boldsymbol{u}, \\
&F_{21}(\boldsymbol{u}, \boldsymbol{v}) = \boldsymbol{u} \odot A_x \boldsymbol{v}, \quad F_{22}(\boldsymbol{v}) = \boldsymbol{v} \odot A_y \boldsymbol{v}; \quad F_{23}(\boldsymbol{\phi}) = \frac{1}{2}\boldsymbol{\phi} \odot A_y \boldsymbol{\phi}, \\
&F_{31}(\boldsymbol{u}, \boldsymbol{\phi}) = \frac{1}{2}\boldsymbol{\phi} \odot A_x \boldsymbol{u}, \quad F_{32}(\boldsymbol{u}, \boldsymbol{\phi}) = \boldsymbol{u} \odot A_x \boldsymbol{\phi}, \\
&F_{33}(\boldsymbol{v}, \boldsymbol{\phi}) = \frac{1}{2}\boldsymbol{\phi} \odot A_y \boldsymbol{v}, \quad F_{34}(\boldsymbol{v}, \boldsymbol{\phi}) = \boldsymbol{v} \odot A_y \boldsymbol{\phi},
\end{aligned}
\tag{21}
$$

where $A_x, A_y \in \mathbb{R}^{n_{xy} \times n_{xy}}$ are constant coefficient matrices for discrete first-order and second-order differential operators which incorporate the boundary conditions.

The numerical scheme was implemented in Fortran and uses a sparse matrix environment. For operations with sparse matrices we employed SPARSEKIT library Saad [55] and the sparse linear systems obtained during the quasi-Newton iterations were solved using MGMRES library Barrett et al. [9], Kelley [40], Saad [56]. Here we didn't decouple the model equations like in Stefanescu and Navon [60] where the Jacobian is either block cyclic tridiagonal or block tridiagonal. By keeping all discrete equations together the corresponding SWE adjoint model can be solved with the same implicit scheme used for forward model. Moreover, we employed 10 nonlinear terms in (18) in comparison with only 6 in [60, 61] to obtain more accurate forward and adjoint POD/DEIM reduced order model solutions. The discrete tangent linear and adjoint models were derived by hand. At the end of the present manuscript there is an appendix formally describing the tangent linear and adjoint ADI SWE models.

5.2 SWE 4D-Var data assimilation reduced order systems

To reduce the computational cost of 4D-Var SWE data assimilation we propose three different POD based reduced order 4D-Var SWE systems depending on standard POD, tensorial POD and standard POD/DEIM reduced order methods discussed in Stefanescu et al. [61]. These three ROMs treat the nonlinear terms in a different manner (see equations (6),(7),(8)) while reduced Jacobian computation is done analytically for all three approaches.

Tensorial POD and POD/DEIM nonlinear treatment make use of an efficient decoupling of the full spatial variables from reduced variables allowing most of the calculations to be performed during the off-line stage while standard POD don't. However, computation of tensors such as T in (7) is required by all three ROMs in the off-line stage since the analytic reduced Jacobian on-line calculations depend on them. Clearly, standard POD is advantaged since usually the reduced Jacobians are obtained by projecting the full Jacobians onto POD spaces during on-line stage so two computational costly operations are avoided.

Since all ROMs are using exact reduced Jacobians the corresponding adjoint models have the same computational complexity. POD/DEIM backward in time reduced model relies on approximate tensors calculated with the algorithm introduced in [61, p.7] while the POD adjoint models compute the tensors exactly. For POD/DEIM approach this leads to slightly different reduced Jacobians in comparison with the ones calculated by standard and tensorial POD leading to different adjoint models. Still, nonlinear POD/DEIM approximation (8) is accurate and agrees with standard POD (6) and tensorial POD representations (7). Standard and Tensorial POD have the same adjoint models.

With these differences in mind we are now ready to describe the algorithms behind each reduced data assimilation systems for a Galerkin projection and the POD basis shares information of both forward and adjoint trajectories. For POD/DEIM SWE data assimilation algorithm we describe only the off-line part since the on-line and decisional stages are generical presented in the tensorial and standard POD reduced data assimilation algorithms.

Algorithm 1 Standard and Tensorial POD SWE DA systems

Off-line stage

1: Generate background state $\mathbf{u}$, $\mathbf{v}$ and $\boldsymbol{\phi}$.
2: Solve full forward ADI SWE model to generate state variables snapshots.
3: Solve full adjoint ADI SWE model to generate adjoint variables snapshots.
4: For each state variable compute a POD basis using snapshots describing dynamics of the forward and its corresponding adjoint trajectories.
5: Compute tensors as T in (7) required for reduced Jacobian calculations. Calculate other POD coefficients corresponding to linear terms.

On-line stage - Minimize reduced cost functional $\mathcal{J}^{\text{POD}}$ (10a)

6: Solve forward reduced order model (13a).
7: Solve adjoint reduced order model (13b).
8: Compute reduced gradient (13c).

Decisional stage

9: Project the suboptimal reduced initial condition generated by the on-line stage and perform steps 1 and 2 of off-line stage. Using full forward information evaluate J in (1a). If $\|\mathcal{J}\| > \varepsilon_3$ then continue the off-line stage from step 3, otherwise STOP.

The on-line stages of all reduced data assimilation systems correspond to minimization of the cost function $\mathcal{J}^{\text{POD}}$ performed on a reduced POD manifold. Thus, the on-line stage is also referred as inner phase or reduced minimization cycle. The stoping criteria are

$$\|\nabla \mathcal{J}^{\text{POD}}\| \leq \varepsilon_1, \quad \|\mathcal{J}^{\text{POD}}_{(i+1)} - \mathcal{J}^{\text{POD}}_{(i)}\| \leq \varepsilon_2, \quad \text{No of function evaluations} \leq \text{MXFUN}, \tag{22}$$

Algorithm 2 POD/DEIM SWE DA systems

Off-line stage

1: Generate background state $\mathbf{u}$, $\mathbf{v}$ and $\boldsymbol{\phi}$.
2: Solve full forward ADI SWE model to generate nonlinear terms and state variables snapshots.
3: Solve full adjoint ADI SWE model to generate adjoint variables snapshots.
4: For each state variable compute a POD basis using snapshots describing dynamics of the forward and its corresponding adjoint trajectories. For each nonlinear term compute a POD basis using snapshots from the forward model.
5: Compute discrete empirical interpolation points for each nonlinear term.
6: Calculate other linear POD coefficients and POD/DEIM coefficients as $W^TV(P^TV)^{-1}$ in (8).
7: Compute tensors such as T using algorithm described in [61, p.7] required for reduced Jacobian calculations.

where $J_{(i)}^{POD}$ is the cost function evaluation at inner iteration (i) and MXFUN is the number of function evaluations allowed during one reduced minimization cycle.

The off-line stage is also called an outer iteration even if no minimization is performed during this phase. However it includes a general stopping criterion for reduced data assimilation system $\|\mathcal{J}\| \leq \varepsilon_3$ where $\mathcal{J}$ is computed using same formulation as the full data assimilation cost function (1a) since forward full information is available.

6 Numerical results

This section is divided in two parts. The first one focuses on POD basis construction strategies and tensorial POD SWE 4D-Var is used for conclusive numerical experiments while the second part measures the performances of the three proposed reduced order SWE data assimilation systems.

In our numerical experiments, we apply 10% uniform perturbations on the initial conditions of Grammeltvedt [27] and generate twin-experiment observations at every grid space point location and every time step. We use the following constants $L = 6000km,\ D = 4400km,\ \hat{f} = 10^{-4}s^{-1},\ \beta = 1.5 \cdot 10^{-11}s^{-1}m^{-1},\ g = 10ms^{-2},\ H_0 = 2000m,\ H_1 = 220m,\ H_2 = 133m$.

We did not choose random perturbations since a fair comparison between each reduced optimization strategies discussed in this study is desired. The background state is computed using a 5% perturbations of the initial conditions. The background and observation error covariance matrices are taken to be identity matrices. The length of the assimilation window is selected to be $3h$.

The BFGS optimization method option contained in the CONMIN software (Shanno and Phua [59]) is employed for high-fidelity full SWE 4-D VAR as well as all variants of reduced SWE 4D-Var data assimilation systems. BFGS uses a line search method which

is globally convergent in the sense that $lim_{k\to\infty}\|\nabla\mathcal{J}^{(k)}\| = 0$ and utilizes approximate Hessians to include convergence to a local minimum.

In all our reduced data assimilation experiments we use $\varepsilon_1 = 10^{-14}$ and $\varepsilon_2 = 10^{-5}$ which are important for the reduced minimization (on-line stage) stopping criteria defined in (22). For the full data assimilation experiment we used only $\|\nabla\mathcal{J}\| \leq 10^{-14}$ and $\|\mathcal{J}\| \leq \varepsilon_3$. We do not define here ε_3 and MXFUN since they may vary from one numerical test to another.

All reduced data assimilation systems employ Galerkin projection to construct their low-rank approximation POD models.

6.1 Choice of POD basis

The tensorial POD reduced SWE data assimilation is selected to test which of the POD basis snapshots selection strategies perform better with respect to suboptimal solution accuracy and cost functional decrease. The "adjoint of reduced forward model" approach is compared with "adjoint of reduced forward model + reduced order adjoint model" method discussed in section 4.

For AR approach there is no need for implementing the full adjoint SWE model since the POD basis relies only on forward trajectories snapshots. Consequently its off-line stage will be computational cheaper in comparison with the similar stage of ARRA approach where adjoint model snapshots are considered inside the POD basis. For this experiment we select 31×23 mesh points and use 50 POD basis functions. MXFUN is set to 25. The singular values spectrums are depicted in Figure 1.

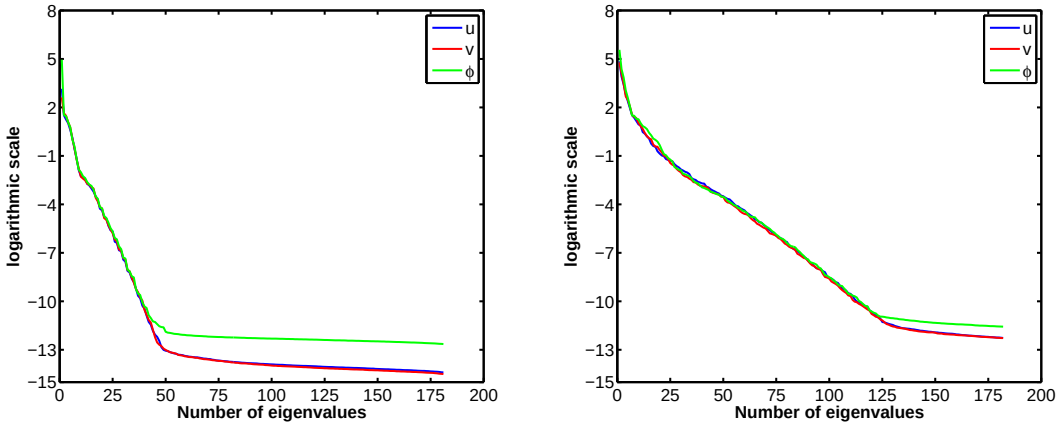

(a) Forward model snapshots only

(b) Forward and adjoint models snapshots

Figure 1: The decay around of the singular values of the snapshots solutions for u, v, ϕ for $\Delta t = 960s$ and integration time window of $3h$.

Forward snapshots consist in "predictor" and "corrector" state variables solutions $\boldsymbol{w}^{t_{i+1/2}}$, $\boldsymbol{w}^{t_i}$, $i = 0, 1, .., t_f - 1$ and $\boldsymbol{w}^{t_f}$ obtained by solving the two steps forward ADI

SWE model. The adjoint snapshots include the "predictor" and "corrector" adjoint solutions $\lambda_{\mathbf{w}}^{t_{i-1/2}}$, $\lambda_{\mathbf{w}}^{t_i}$, $i = 1, 2, ., t_f$ and $\lambda_{\mathbf{w}}^{t_0}$ as well as other two additional intermediary solutions computed by the full adjoint model. An appendix is included providing details about the ADI SWE forward and adjoint models equations. Table 1 presents the POD truncation average absolute errors for AR and ARRA approaches for both forward and adjoint initial conditions.

	AR	ARRA
E_u	2.39e-15	1.39e-6
E_v	8.16e-16	7.54e-7
E_ϕ	2.75e-13	1.59e-6

	AR	AR+RA
E_{λ_u}	207.38	1.71e-6
E_{λ_v}	138.40	7.91e-7
E_{λ_ϕ}	199.377	1.23e-6

Table 1: Average absolute errors of forward (left) and adjoint (right) tensorial POD SWE initial conditions using AR and ARRA approaches.

Even if AR reduced data assimilation does not require a full adjoint model we chose to display the reduced adjoint average absolute error as a measure of increased probability that the output local minimum is far away from the local minimum computed with the high-fidelity configuration. Figure 2 depicts the minimization performances of the tensorial POD SWE 4D-Var systems using different set of snapshots in comparison with the output of the full space ADI SWE 4D-Var system. The cost function and gradient values are normalized by dividing them with their initial values.

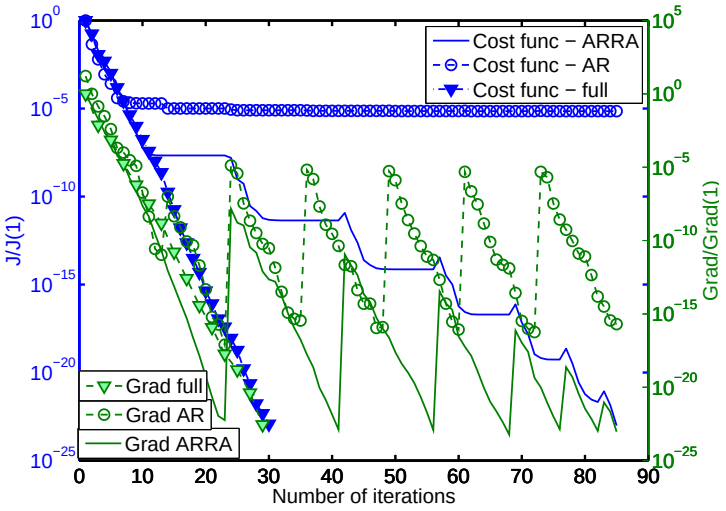

Figure 2: Tensorial POD/4DVAR ADI 2D Shallow water equations – Evolution of cost function and gradient norm as a function of the number of minimization iterations. The information from the adjoint equations has to be incorporated into POD basis.

Clearly the best POD basis construction strategy is "adjoint of reduced forward model + reduced order adjoint model" approach since the corresponding tensorial POD SWE

4D-Var achieved a cost function reduction close to the one obtained by the high-fidelity ADI SWE 4D-Var. One can notice that 6 POD bases recalculations were required to achieve the suboptimal solution since 6 plateaus regions followed by 6 peaks are visible on the cost function curve. If only forward trajectory snapshots are utilized for POD basis construction the cost function decay is modest indicating only 5 orders of magnitude decrease despite of carrying out 13 POD bases updates. This underlines that the "adjoint of reduced forward model" approach is not able to represent well the controlled dynamics in its reduced manifold leading to an suboptimal cost function value of $0.48e{+}02$. In the case of "adjoint of reduced forward model + reduced order adjoint model" strategy the suboptimal cost function value is $0.48e$-14 while the optimal cost function calculated by the high fidelity ADI SWE 4D-Var system is $0.65e$-16. Two additional measures of the minimization performances are presented in Table 2 where the relative errors of tensorial POD suboptimal solutions with respect to observations and optimal solution are displayed.

	AR	ARRA
E_u^*	$1.57e$-2	$5.19e$-11
E_v^*	$1.81e$-2	$6.77e$-11
$E_\phi*$	$1.6e$-2	$5.96e$-11

	AR	ARRA
E_u^o	$6.69e$-5	$2.39e$-11
E_v^o	$2.29e$-4	$8.71e$-11
E_ϕ^o	$1.08e$-6	$3.7e$-13

Table 2: Relative errors of suboptimal solutions of reduced tensorial POD SWE systems using different snapshot sets and optimal solution (left) and observations (right). * denotes errors with respect to the optimal solution obtained using high-fidelity ADI SWE 4D-Var SWE system while ^{o} characterizes errors with respect to the observations.

We conclude by stating that information of the full adjoint and forward equations must be included together in the snapshots set used to derive the POD basis for Galerkin based POD reduced order models thus assuring better representations of the controlled variables during the reduced optimization process. Next subsection includes experiments using only ARRA strategy.

6.2 Reduced order POD based SWE 4D-Var data assimilation systems

This subsection is devoted to numerical experiments of the reduced SWE 4D-Var data assimilation systems introduced in subsection 5.2 using POD based models and discrete empirical interpolation method. In the on-line stage tensorial POD and POD/DEIM SWE forward models were shown to become faster than standard POD SWE forward model being $76\times$ and $450\times$ more efficient for more than $300,000$ variables (Stefanescu et al. [61]). Moreover, a tensorial based algorithm was developed in [61] allowing the POD/DEIM SWE model to compute its off-line stage faster than the standard and tensorial POD approaches despite additional SVD calculations and other reduced coefficients calculations.

Consequently, there are good expectations to assume that POD/DEIM SWE 4D-Var system would deliver suboptimal solutions faster than the other standard and tensorial POD data assimilation systems. The reduced Jacobians needed for solving the forward and adjoint reduced models are computed analytically for all three approaches. Since the derivatives computational complexity do not depend on full space dimension the corresponding adjoint models have similar CPU time costs. Thus, most of the CPU time differences will arise from the on-line stage of the reduced forward models and their off-line requirements.

Using nonlinear POD/DEIM approximation introduced in (8) we implement the reduced forward POD/DEIM SWE obtained by projecting the ADI SWE equations onto the POD subspace. Then the reduced optimality conditions (13) are computed. The POD/DEIM reduced adjoint SWE model has a similar structure as full adjoint SWE model requiring two different linear algebraic systems of equations to be solved at each time level. The first reduced optimization test is performed for a mesh of 31×23 points, a POD basis dimension of $k = 50$, and 50 and 180 DEIM interpolation points are used. We obtain a cost function decrease of only 5 orders of magnitude after 10 POD bases updates and imposing a relaxed threshold of MXFUN = 100 function evaluations per inner loop reduced optimization (see Figure 3a).

Next we decrease the spatial resolution to 17×13 points and perform the reduced optimization with increasing number of DEIM points and MXFUN = 20 (see Figure 3b). For $m = 165$, POD/DEIM nonlinear terms approximations are identical with standard POD representations since the boundary variables are not controlled. We notice that even for $m = 135$ there is an important loss of performance since the cost function decreases by only 10^{-12} orders of magnitude in 178 inner iterations while for $m = 165$ (standard POD) the cost functions achieves a 10^{-23} orders of magnitude decrease in only 52 reduced optimization iterations. The initial level of root mean square error (RMSE) inflicted by truncation of POD expansion for $k = 50$ and for a number of DEIM interpolation points $m = 50$ at final time $t_f = 3h$ are similar for all reduced order methods (see Table 3). It means that some of the nonlinear POD/DEIM approximations are more sensible to changes in initial data during the optimization course while their nonlinear tensorial and standard POD counterparts proved to be more robust.

	POD/DEIM	tensorial POD	standard POD
E_u	1.21e-7	1.2e-7	1.2e-7
E_v	7.6e-8	7.48e-8	7.48e-8
E_ϕ	1.4e-7	1.36e-7	1.36e-7

Table 3: RMSE of reduced order solutions of the forward SWE ROMS with respect to the full space ADI SWE state variables at final time $t_f = 3h$ for the same initial conditions used for snapshots and POD basis generations. Number of mesh points is $n = 17 \times 13$, number of POD basis functions is $k = 50$ and number of DEIM points is $m = 50$.

We verify the implementation of the POD/DEIM SWE 4D-Var system and good

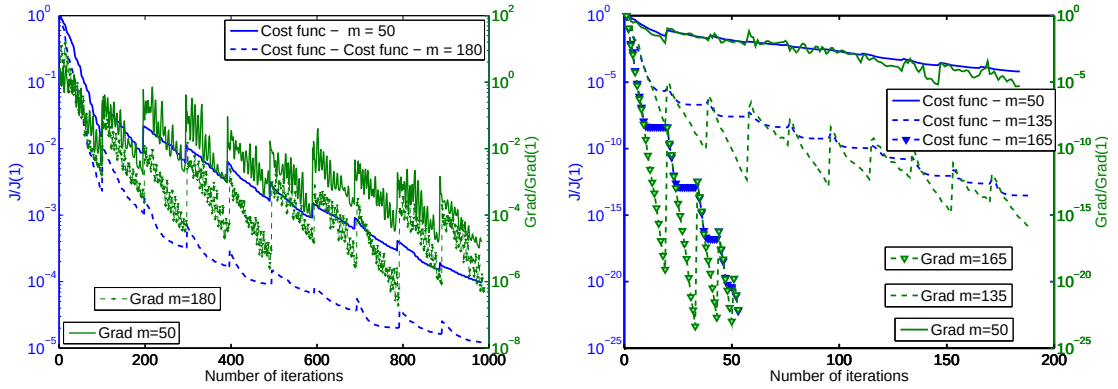

(a) Number of mesh points 31×23 (b) Number of mesh points 17×13

Figure 3: Standard POD/DEIM ADI SWE 4D-Var system – Evolution of cost function and gradient norm as a function of the number of minimization iterations for different number of mesh points and various number of DEIM points.

results are obtained for standard gradient and adjoint tests in Figure 4a. Then we begin checking the accuracy of the POD/DEIM nonlinear terms during the optimization and compare them with the similar tensorial POD nonlinear terms (7). We found out that POD/DEIM nonlinear terms involving height $\boldsymbol{\phi}$, i.e. $\tilde{F}_{12}$, $\tilde{F}_{23}$, $\tilde{F}_{31}$, $\tilde{F}_{33}$ lose $2-3$ orders accuracy in comparison with tensorial nonlinear terms. Thus we replaced only these terms by their tensorial POD representations and the new hybrid POD/DEIM SWE system using 50 DEIM interpolation points reached the expected performances (see Figure 4b).

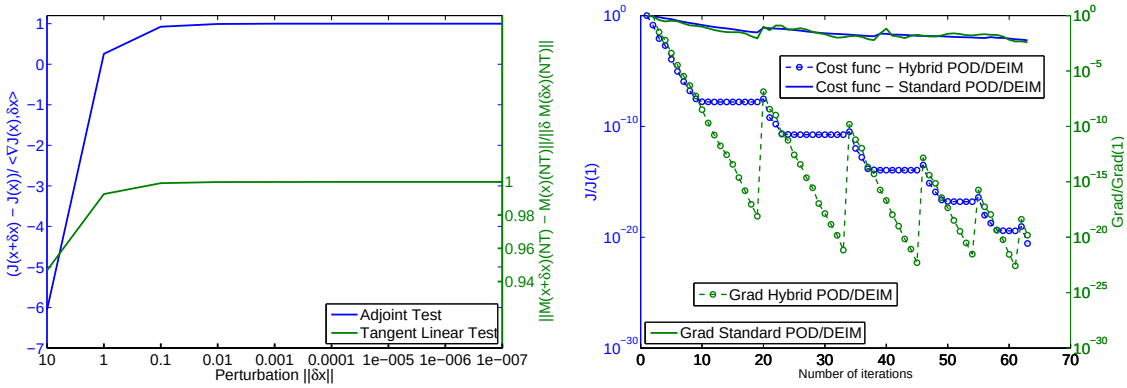

(a) Tangent Linear and Adjoint test (b) Cost function and gradient decays

Figure 4: Tangent linear and adjoint test for standard POD/DEIM SWE 4D-Var system. Optimization performances of Standard POD/DEIM and Hybrid POD/DEIM 4D-Var ADI 2D shallow water equations for $n = 17 \times 13$.

Next we test the new hybrid POD/DEIM reduced data assimilation system using different POD basis dimensions and various numbers of DEIM points. For ROM optimization to deliver accurate suboptimal surrogate solutions similar to the output of full optimization one must increase the POD subspace dimension (see Figure 5a) for large number of mesh points configurations. This will definitely lead to slow reduced data assimilation systems being in contradiction with the concept of reduced order modeling. For $k \geq 50$ we notice similar performances so in our next numerical experiments we set POD basis with dimensions k no larger then 50. Then we tested different configurations of DEIM points and for values of $m \geq 30$ the reduced optimization results are almost the same in terms of cost function decreases. Our findings are confirmed also by the relative errors accuracy of the suboptimal hybrid POD/DEIM SWE 4D-Var solutions with respect to the optimal solutions computed using high-fidelity ADI SWE 4D-Var system and observations (see Tables 4,5).

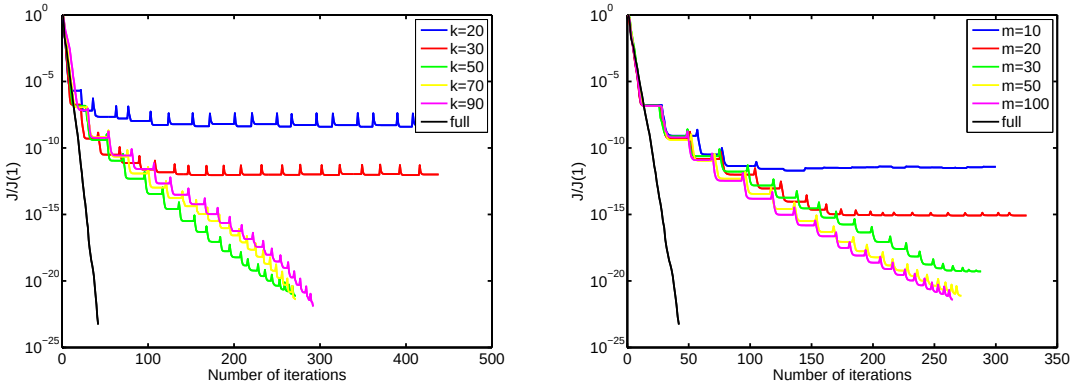

(a) Number of DEIM points $m = 50$ (b) Number of POD basis dimension $k = 50$

Figure 5: Performances of hybrid POD/DEIM SWE DA system with various values of POD basis dimensions (a) and different number of interpolation points (b). The spatial configuration uses $n = 61 \times 45$ and maximum number of function evaluation per inner iteration is set MXFUN= 30.

	$k = 20$	$k = 30$	$k = 50$	$k = 70$	$k = 90$	Full
E_u^o	1.03e-4	1.57e-6	4.1e-11	3.75e-11	2.1e-11	2.77e-12
E_v^o	4.04e-4	6.29e-6	1.72e-10	1.16e-10	8.55e-11	1.27e-11
E_ϕ^o	2.36e-6	3.94e-8	1.09e-12	6.78e-13	2.3e-13	5.79e-14

Table 4: Relative errors of suboptimal hybrid POD/DEIM SWE 4D-Var solutions with respect to observations. The number of DEIM interpolation points is hold constant $m = 50$ while k is varied.

The last part of the present subsection is dedicated to performance comparisons between proposed optimization systems using reduced and full space configurations.

	$m = 10$	$m = 20$	$m = 30$	$m = 50$	$m = 100$	Full
E_u^o	4.28e-6	4.91e-8	4.15e-10	4.1e-11	3.08e-11	2.77e-12
E_v^o	6.88e-6	1.889e-7	1.54e-9	1.72e-10	1.25e-10	1.27e-11
E_ϕ^o	7.15e-8	1.04e-9	7.79e-12	1.09e-13	7.39e-13	5.79e-14

Table 5: Relative errors of suboptimal hybrid POD/DEIM SWE 4D-Var solutions with respect to observations. Different DEIM interpolation points are tested and k is hold constant 50.

We use different numbers of mesh points resolutions namely, 31×23, 61×45, 101×71, 121×189, 151×111 resulting in 1823, 7371, 20493, 28971 and 48723 control variables respectively. Various values of maximum number of function evaluations per each reduced minimization are also tested. We already saw that for increased number of POD basis dimensions the reduced data assimilation 4D-Var system leads to a cost function decrease almost similar with the one obtained by the full SWE 4D-Var system (see Figure 5a). Thus we are more interested to measure how fast the proposed data assimilation systems can reach the same threshold ε_3 in terms of cost function rate of decay.

The next experiment uses the following configuration: $n = 61 \times 45$ space points, number of POD basis modes $k = 50$, MXFUN = 10 and $\varepsilon_3 = 10^{-7}$. Figure 6 depicts the cost function evolution during hybrid POD/DEIM SWE 4D-Var, standard POD SWE 4D-Var and tensorial POD SWE 4D-Var minimizations versus number of iterations and CPU times. We notice that for 50 DEIM points the hybrid POD/DEIM DA system requires 3 additional POD basis updates to decrease the cost functional value bellow 10^{-7} in comparison with standard and tensorial POD DA systems. By increasing the number of DEIM points to 120 the number of required POD basis recalculations is decreased by a factor of 2 and the total number of reduced minimization iterations is reduced by 20. The hybrid POD/DEIM SWE 4D-Var system using $m = 120$ is faster with $\approx 37s$ and $\approx 86s$ than both the tensorial and standard POD SWE 4D-Var systems.

Next we increase the number of spatial points to $n = 151 \times 111$ and use the same POD basis dimension $k = 50$. MXFUN is set to 15. The stopping criteria for all optimizations is $\|\mathcal{J}\| < \varepsilon_3 = 10^{-1}$. All the reduced order optimizations required two *POD* basis recalculations and the hybrid POD/DEIM SWE 4D-Var needed one more iteration than the standard and tensorial POD systems (see Figure 7a). In this case the hybrid POD/DEIM SWE 4D-Var system is not so sensitive to the number of DEIM points as seen in the previous experiment. The hybrid POD/DEIM SWE 4D-Var system using $m = 30$ is faster with $\approx 9s, 92s, 781s, 4674s$ (by 1.01, 1.15, 2.31, 8.86 times) than the hybrid POD/DEIM ($m = 50$), tensorial POD, standard POD and full SWE 4D-Var data assimilation systems respectively (see Figure 7b).

Table 6 displays the CPU times required by all the optimization methods to decrease the cost function values below a specific threshold ε_3 specific to each space configuration (row 2 in table 6). The POD basis dimension is set to $k = 30$. The bold values correspond to the best CPU time performances and some important conclusions can be

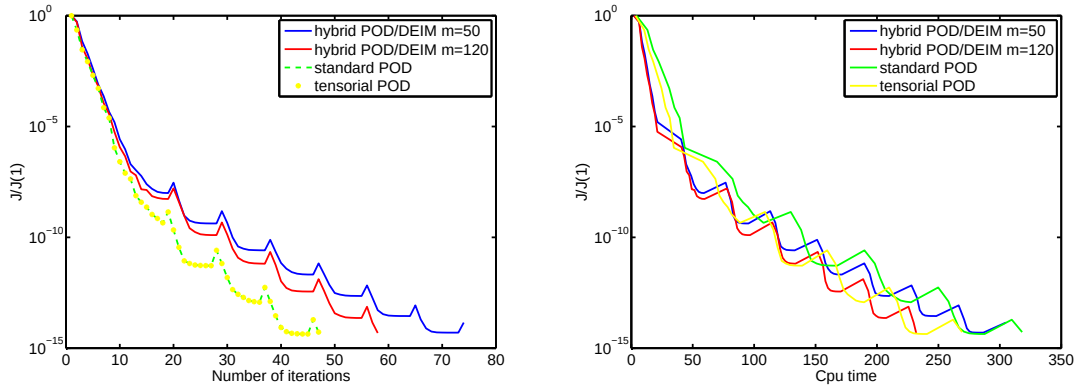

(a) Iteration performance (b) Time performance

Figure 6: Number of minimization iterations and CPU time comparisons for the reduced order SWE DA systems vs. full SWE DA system. The spatial configuration uses $n = 61 \times 45$ and maximum number of function evaluation per inner iteration is set MXFUN= 10.

drawn. There is no need for use of reduced optimization for $n = 31 \times 23$ or less since the full data assimilation system is faster. The hybrid POD/DEIM SWE 4D-Var using 50 DEIM points is the most rapid optimization approach for numbers of space points larger than 61×45. For $n = 151 \times 111$ it is 1.23, 2.27, 12.329 faster than tensorial POD, standard POD and full SWE 4D-Var systems. We also notice that the CPU time speedup rates are directly proportional with the increase of the full space resolution dimensions.

Space points	31×23	61×45	101×71	121×89	151×111
ε_3	$\|J\| < 1.e\text{-}09$	$\|J\| < 5.e\text{-}04$	$\|J\| < 1.e\text{-}01$	$\|J\| < 5$	$\|J\| < 1e{+}03$
hybrid DEIM 50	48.771	**63.345**	**199.468**	**358.17**	**246.397**
hybrid DEIM 120	44.367	64.777	210.662	431.460	286.004
standard POD	63.137	131.438	533.052	760.462	560.619
tensorial POD	54.54	67.132	216.29	391.075	303.95
FULL	**10.6441**	117.02	792.929	1562.3425	3038.24

Table 6: CPU time for reduced optimization and full 4D-Var sharing the same stoping criterion $\|J\| < \varepsilon_3$. Number of POD modes is selected 30 and MXFUN = 15.

Next we increased the POD basis dimension k to 50 and the corresponding CPU times are described in Table 7. Notice also that ε_3 values are decreased. The use of reduced optimization system is justified for $n > 61 \times 45$ where the hybrid POD/DEIM DA system using different numbers of DEIM points proves to be the fastest choice. For 151×111 space points the hybrid POD/DEIM reduced optimization system is 1.15, 2.31, and 8.86 times faster than tensorial POD, standard POD and full SWE 4D-Var systems respectively.

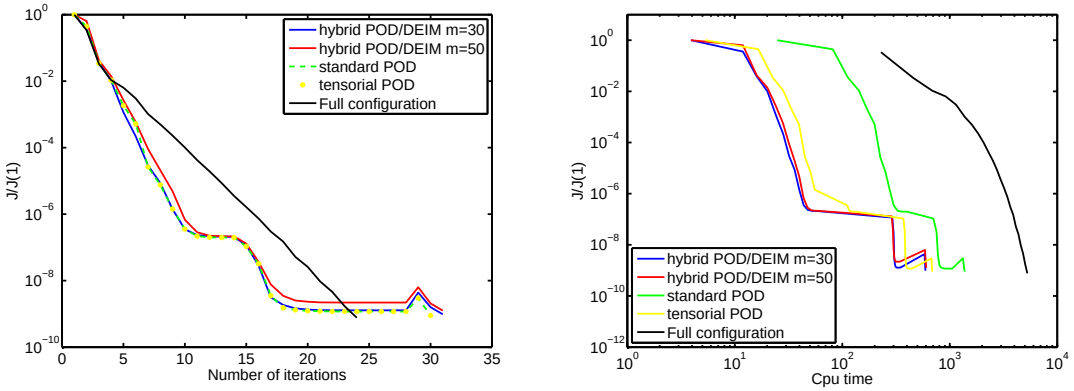

(a) Iteration performance (b) Time performance

Figure 7: Number of iterations and CPU time comparisons for the reduced order SWE DA systems vs. full SWE DA system. The spatial configuration uses $n = 151 \times 111$ and maximum number of function evaluation per inner iteration is set MXFUN= 15.

Space points	31×23	61×45	101×71	121×89	151×111
ε_3	$\|J\| < 1.e\text{-}14$	$\|J\| < 1.e\text{-}07$	$\|J\| < 1.e\text{-}04$	$\|J\| < 5e\text{-}03$	$\|J\| < 1e\text{-}01$
hybrid DEIM 30	214.78	288.627	593.357	**499.676**	**594.04**
hybrid DEIM 50	211.509	246.65	**529.93**	512.721	603.21
standard POD	190.572	402.208	1243.234	1315.573	1375.4
tensorial POD	269.08	311.106	585.509	662.95	685.57
FULL	**14.1005**	**155.674**	1057.715	2261.673	5268.7

Table 7: CPU time for reduced optimization and full 4D-Var sharing the same stoping criterion $\|J\| < \varepsilon_3$. Number of POD modes is selected 50 and MXFUN = 15.

Now we are able to describe the computational time required by each step of the high-fidelity and reduced optimization systems. We are using 151×111 space points, POD basis dimension $k = 50$, and number of DEIM points $m = 30$. MXFUN is set to 15 and $\varepsilon_3 = 10^{-1}$. For the full space 4D-Var system the line search and Hessian approximations are computational costly and are described separately (see table 8) while for reduced data assimilation systems these costs are very small being included in the reduced adjoint model CPU time.

The most expensive part of the Hybrid POD/DEIM 4D-Var optimization process (see table 9) occurs during the off-line stage and consists in the snapshots generation stage where the full forward and adjoint models are integrated in time. This is valid also for tensorial POD 4D-Var DA system (table 10) while in the case of standard POD 4D-Var system (table 11) the on-line stage is far more costly since the computational complexity of the corresponding reduced forward model still depends on the full space dimension.

The algorithm proposed in Stefanescu and Navon [60, p.16] utilizes DEIM interpolation points, explores the structure of polynomial nonlinearities and delivers fast tensorial

Process	Time	#	Total
Solve full forward model	$\approx$ 80s	26x	$\approx$ 2080s
Solve full adjoint model	$\approx$ 76.45s	26x	$\approx$ 1987.7s
Other (Line Search, Hessian approx)	$\approx$ 46.165	26x	$\approx$ 1200.3s
Total full 4D-Var			$\approx$ 5268s

Table 8: The calculation times for solving the optimization problem using full 4D-Var for a number of mesh points of 151×111. Stoping criterion $\|\mathcal{J}\| < 10^{-1}$ is set.

Process	Time	#	Total
Off-line stage			
Solve full forward model + nonlinear snap.	$\approx$ 80.88s	2x	$\approx$ 161.76s
Solve full adjoint model + nonlinear snap.	$\approx$ 76.45s	2x	$\approx$ 152.9s
SVD for state variables	$\approx$ 53.8	2x	$\approx$ 107.6s
SVD for nonlinear terms	$\approx$ 11.57	2x	$\approx$ 23.14s
DEIM interpolation points	$\approx$ 0.115	2x	$\approx$ 0.23s
POD/DEIM model coefficients	$\approx$ 1.06	2x	$\approx$ 2.12s
tensorial POD model coefficients	$\approx$ 8.8	2x	$\approx$ 17.6s
On-line stage			
Solve ROM forward	$\approx$ 2s	33x	$\approx$ 66s
Solve ROM adjoint	$\approx$ 1.9s	33x	$\approx$ 62.69s
Total Hybrid POD/DEIM 4D-Var			$\approx$ 594.04s

Table 9: The calculation times for solving the optimization problem using Hybrid POD/DEIM 4D-Var for a number of mesh points of 151×111, POD basis dimension $k = 50$ and 30 DEIM interpolation points.

calculations of POD/DEIM model coefficients. Consequently the hybrid POD/DEIM SWE 4D-Var systems has the fastest off-line stage among all proposed reduced data assimilation systems despite additional SVD calculations and other reduced coefficients computations.

For all three reduced optimization systems the Jacobians are calculated analytically and their computations depend only on the reduced space dimension k. As a consequence, all the adjoint models have the same computational complexity and in the case of hybrid POD/DEIM SWE 4D-Var the on-line Jacobians computations rely partially on approximate tensors calculated during the off-line stage while in the other two reduced order data assimilation systems exact tensorial POD model coefficients are used.

It is clear that the reduced optimization data assimilation systems become slow if it is often required to project back to the high fidelity model and reconstruct the reduced POD subspace. Thus, we compare the CPU times obtained by our reduced data assimilation systems using at most 10, 15, and 20 function evaluations per reduced minimization cycle. The results for $k = 30$ (see Table 12) shows that no more than 15 function evaluations should be allowed for each reduced minimization cycle and hybrid

Process	Time	#	Total
Off-line stage			
Solve full forward model + nonlinear snap.	$\approx$ 80s	2x	$\approx$ 160s
Solve full adjoint model + nonlinear snap.	$\approx$ 76.45s	2x	$\approx$ 152.9s
SVD for state variables	$\approx$ 53.8s	2x	$\approx$ 107.6s
tensorial POD model coefficients	$\approx$ 23.735s	2x	$\approx$ 47.47s
On-line stage			
Solve ROM forward	$\approx$ 4.9s	32x	$\approx$ 156.8s
Solve ROM adjoint	$\approx$ 1.9s	32x	$\approx$ 60.8s
Total Tensorial POD 4D-Var			$\approx$ 685.57s

Table 10: The calculation times for solving the optimization problem using Tensorial POD 4D-Var for a number of mesh points of 151×111, and POD basis dimension $k = 50$.

Process	Time	#	Total
On-line stage			
Solve ROM forward	$\approx$ 26.523s	32x	$\approx$ 846.72s
Solve ROM adjoint	$\approx$ 1.9	32x	$\approx$ 60.8s
Total Standard 4D-Var			$\approx$ 1375.4s

Table 11: The calculation times for on-line stage of Standard POD 4D-Var for a number of mesh points of 151×111 and POD basis dimension $k = 50$. The off-line stage is identical with the one in Tensorial POD 4D-Var system.

POD/DEIM data assimilation system using 30 interpolation points provides the fastest solutions. While for 101×71 number of space points 15 function evaluation are required, for other spatial configurations MXFUN = 10 is sufficient.

Space points	MXFUN	ε_3	DEIM points	Method
31×23	-	$1.e$-9	-	Full
61×45	10	$5.e$-04	30	Hybrid POD/DEIM
101×71	15	$1.e$-01	30	Hybrid POD/DEIM
121×89	10	5	30	Hybrid POD/DEIM
151×111	10	$1e$+03	30	Hybrid POD/DEIM

Table 12: The fastest optimization data assimilation systems for various number of spatial points, different MXFUN values and number of DEIM points. Number of POD modes is $k = 30$.

For POD basis dimension $k = 50$, we discover that more function evaluations are needed during the inner reduced minimizations in order to obtain the fastest CPU times and MXFUN should be set to 15. More DEIM points are also required as we notice in Table 13.

We conclude that hybrid POD/DEIM SWE 4D-Var system delivers the fastest sub-

Space points	MXFUN	ε_3	DEIM points	Method
31×23	-	1.e-14	-	Full
61×45	-	1.e-7	-	Full
101×71	15	1.e-04	50	Hybrid POD/DEIM
121×89	15	5.e-3	50	Hybrid POD/DEIM
151×111	15	1.e-1	50	Hybrid POD/DEIM

Table 13: The fastest optimization data assimilation systems for various number of spatial points, different MXFUN values and number of DEIM points. Number of POD modes is $k = 50$.

optimal solutions and is far more competitive in terms of CPU time than the full SWE data assimilation system for space resolutions larger than 61×45 points. Hybrid POD/DEIM SWE 4D-Var is at least two times faster than standard POD SWE 4D-Var for $n \geq 101 \times 71$.

In terms of suboptimal solution accuracy, the hybrid POD/DEIM delivers similar results as tensorial and standard POD SWE 4D-Var systems (see tables 14, 15, 16). $E_{\mathbf{w}}$ and $E_{\lambda_{\mathbf{w}}}$ are the initial conditions relative errors of reduced forward and adjoint SWE models with respect to the high fidelity SWE models solutions determined by POD basis truncation. The optimal solution was computed with the full SWE 4D-Var system. To measure the suboptimal solutions accuracy we calculated the relative errors of the initial conditions obtained via reduced optimization apparatus $\mathbf{w}^{\text{POD}}$ and the outcome of the full 4D-Var system $\mathbf{w}^*$. Two different POD bases dimensions were tested $k = 30,\ 50$ and MXFUN was set to 15. We chose $\varepsilon_3 = 10^{-15}$ for all data assimilation systems and only 20 outer iterations were allowed for all reduced 4D-Var optimization systems. For Hybrid POD/DEIM 4D-Var system we used 50 DEIM interpolation points.

n	E_u	E_{λ_u}	hybrid DEIM	sPOD	tPOD
31×23	4.51e-5	5.09e-5	5.86e-8	9.11e-8	9.11e-8
61×45	1.55e-4	2.92e-4	2.4e-5	1.63e-5	1.63e-5
101×71	6.06e-4	6.56e-4	2.03e-4	1.83e-4	1.83e-4
121×89	9.88e-4	1.93e-3	1.16e-3	8.07e-4	8.07e-4
151×111	2.07e-3	2.97e-3	4.02e-3	4.2e-3	4.2e-3

E_u	E_{λ_u}	hybrid DEIM	sPOD	tPOD
1.39e-6	1.87e-6	1.13e-10	2.51e-10	2.51e-10
1.58e-5	1.06e-5	2.16e-7	1.38e-7	1.38e-7
4.51e-5	4.76e-5	7.03e-6	5.14e-6	5.14e-6
7.17e-5	8.e-5	5.62e-5	3.15e-5	3.15e-5
1.02e-4	2.77e-4	1.59e-4	1.05e-4	1.05e-4

Table 14: Suboptimal solution error $\|u^{\text{POD}} - u^*\|$ for velocity component u and POD basis dimension $k = 30$ (left) and $k = 50$ (right). E_u and E_{λ_u} are the corresponding initial conditions POD reduced models errors caused by eigenvector truncations in the POD forward and adjoint expansions. u^* is the full 4D-Var optimal solution.

The suboptimal errors of all reduced optimization systems are well correlated with $E_{\mathbf{w}}$ and $E_{\lambda_{\mathbf{w}}}$ having correlation coefficients higher than 0.85. However the correlation coefficients between reduced adjoint model errors $E_{\lambda_{\mathbf{w}}}$ and suboptimal errors are larger than 0.9 which confirm the a-priori error estimation results of Hinze and Volkwein [32] developed for linear-quadratic optimal problems. It states that error estimates for the adjoint state yield error estimates of the control. Extension to nonlinear-quadratic optimal problems is desired and represents subject of future research. In addition, an

n	E_v	E_{λ_v}	hybrid DEIM	sPOD	tPOD
31×23	3.20e-5	4.06e-5	6.03e-8	9.95e-8	9.95e-8
61×45	3.13e-4	3.21e-4	3.75e-5	2.63e-5	2.63e-5
101×71	9.76e-4	5.71e-4	3.51e-4	2.93e-4	2.93e-4
121×89	1.37e-3	1.70e-3	1.38e-3	1.21e-3	1.21e-3
151×111	1.58-3	1.89e-3	6.21e-3	6.22e-3	6.22e-3

E_v	E_{λ_v}	hybrid DEIM	sPOD	tPOD
7.54e-7	1.10e-6	1.25e-10	4.10e-10	4.10e-10
1.09e-5	9.71e-6	3.03e-7	2.82e-7	2.82e-7
3.05e-5	3.55e-5	8.32e-6	9.45e-6	9.45e-6
7.96e-5	8.12e-5	7.19e-5	6.85e-5	6.85e-5
1.06e-4	1.76e-4	2.95e-4	1.94e-4	1.94e-4

Table 15: Suboptimal solution error $\|v^{\text{POD}} - v^*\|$ for velocity component v and POD basis dimension $k = 30$ (left) and $k = 50$ (right). E_v and E_{λ_v} are the corresponding initial conditions POD reduced models errors caused by eigenvector truncations in the POD forward and adjoint expansions. v^* is the full 4D-Var optimal solution.

n	E_ϕ	E_{λ_ϕ}	hybrid DEIM	sPOD	tPOD
31×23	4.38e-5	4.16e-5	1.12e-7	1.83e-7	1.83e-7
61×45	1.84e-4	4.54e-4	5.63e-5	3.34e-5	3.34e-5
101×71	2.21e-3	3.16e-3	6.60e-4	6.45e-4	6.45e-4
121×89	5.60e-3	4.38e-3	2.88e-3	2.54e-3	2.54e-3
151×111	9.04e-3	1.2e-2	8.54e-3	8.46e-3	8.46e-3

E_ϕ	E_{λ_ϕ}	hybrid DEIM	sPOD	tPOD
1.59e-6	1.04e-6	1.12e-10	2.87e-10	2.87e-10
9.58e-6	9.e-6	1.80e-7	2.37e-7	2.37e-7
3.52e-5	4.49e-5	7.60e-6	1.04e-5	1.04e-5
7.84e-5	1.03e-4	5.56e-5	5.04e-5	5.04e-5
1.8e-4	2.77e-4	2.76e-4	2.75e-4	2.75e-4

Table 16: Suboptimal solution error $\|\phi^{\text{POD}} - \phi^*\|$ for geopotential ϕ and POD basis dimension $k = 30$ (left) and $k = 50$ (right). E_ϕ and E_{λ_ϕ} are the corresponding initial conditions POD reduced models errors caused by eigenvector truncations in the POD forward and adjoint expansions. ϕ^* is the full 4D-Var optimal solution.

a-posteriori error estimation apparatus is required by the hybrid POD/DEIM SWE system to guide the POD basis construction and to efficiently select the number of DEIM interpolation points.

The suboptimal solutions delivered by the ROM DA systems equipped with BFGS algorithm are accurate and comparable with the optimal solution computed by the full DA system. In the future we plan to enrich the reduced data assimilation systems by implementing a trust region algorithm (see Arian et al. [7]). It has an efficient strategy for updating the POD basis and it is well known for its global convergence properties.

7 Conclusions

This work studies reduced order modeling approaches for variational data assimilation problems with nonlinear dynamical models. We propose an efficient POD bases selection strategy that ensures the consistency of the reduced-order Karush Kuhn Tucker conditions with the full-order optimality conditions. This approach provides an accurate low-rank approximation of the adjoint model in addition to an accurate low-rank representation of the forward model.

The specific choice of a reduced basis depends on the type of projection employed to construct reduced order model. In the case of a Petrov-Galerkin projection the test POD basis functions of the forward model coincide with the trial POD basis functions of the adjoint model; and similarly, the adjoint test POD basis functions coincide with the forward trial POD basis functions. It is known that Petrov-Galerkin reduced order

models exhibit severe numerical instabilities, therefore stabilization strategies have to be included with this type of reduced data assimilation system [4, 12]. For the Galerkin projection approach the same basis has to represent accurately both the full forward and the full adjoint models. The Galerkin POD basis is constructed from the dominant eigenvectors of the correlation matrix of the aggregated snapshots of full forward and adjoint model outputs. This reduced bases selection strategy is not limited to POD framework. It extends easily to every type of reduced optimization involving adjoint models and projection-based reduced order methods such the reduced basis approach.

Numerical experiments using tensorial POD SWE 4D-Var data assimilation system based on Galerkin projection and different type of POD bases support the proposed approach. The most accurate suboptimal solutions and the fastest decrease of the cost function are obtained using full forward and adjoint snapshots for POD basis generation. If only forward model information is included into the reduced manifold the cost function associated with the data assimilation problem decreases by five orders of magnitude during the optimization process. Taking into account the adjoint information leads to a decrease of the cost function by twenty orders of magnitude. When adjoint information is included the results of the reduced-order data assimilation system are similar with the ones obtained with the full-order SWE 4D-Var DA system. This highlights the importance of choosing appropriate reduced-order bases.

The work also studies the impact of the choice of reduced order technique on the solution of the inverse problem. We consider for comparison standard POD, tensorial POD and standard POD/DEIM. For the first time POD/DEIM is employed to construct a reduced-order data assimilation system for a geophysical two-dimensional flow model. All reduced-order DA systems employ a Galerkin projection and the reduced-order bases use information from both forward and dual solutions. The POD/DEIM approximations of several nonlinear terms involving the height field partially lose their accuracy during the optimization. It suggests that POD/DEIM reduced nonlinear terms are sensitive to input data changes and the selection of interpolation points is no longer optimal. On-going research focuses on increasing the robustness of DEIM for optimization applications. The reduced POD/DEIM approximations of the aforementioned nonlinear terms are replaced with tensorial POD representations. This new hybrid POD/DEIM SWE 4D-Var DA system is accurate and faster than other standard and tensorial POD SWE 4D-Var systems. Numerical experiments with various POD basis dimensions and numbers of DEIM points illustrate the potential of the new reduced-order data assimilation system to reduce CPU time.

For a full system spatial discretization with 151×111 grid points the hybrid POD/DEIM reduced data assimilation system is approximately ten times faster then the full space data assimilation system. This rate increases in proportion to the full mesh size. Hybrid POD/DEIM SWE 4D-Var is at least two times faster than standard POD SWE 4D-Var for numbers of space points larger or equal to 101×71. This illustrates the power of DEIM approach not only for reduced-order forward simulations but also for reduced-order optimization.

Future work of the authors will focus on a generalized DEIM framework to approx-

imate operators since faster reduced Jacobian computations will further decrease the computational complexity of POD/DEIM reduced data assimilation systems. We intend to extend our reduced-order data assimilation systems by implementing a trust region algorithm to guide the re-computation of the bases. On-going work of the authors seeks to develop a-priori and a-posteriori error estimates for the reduced-order optimal solutions, and to use a-posteriori error estimation apparatus to guide the POD basis construction and to efficiently select the number of DEIM interpolation points.

Acknowledgments

The work of Dr. Răzvan Stefanescu and Prof. Adrian Sandu was supported by the NSF CCF–1218454, AFOSR FA9550–12–1–0293–DEF, AFOSR 12-2640-06, and by the Computational Science Laboratory at Virginia Tech. Prof. I.M. Navon acknowledges the support of NSF grant ATM-0931198.

References

[1] K. Afanasiev and M. Hinze. Adaptive Control of a Wake Flow Using Proper Orthogonal Decomposition. Lecture Notes in Pure and Applied Mathematics, 216: 317–332, 2001.

[2] M.U. Altaf, M.E. Gharamti, A.W. Heemink, and I. Hoteit. A reduced adjoint approach to variational data assimilation. Computer Methods in Applied Mechanics and Engineering, 254:1–13, 2013.

[3] M. Ambrozic. A Study of Reduced Order 4D-VAR with a Finite Element Shallow Water Model. Master's thesis, Delft University of Technology, Netherlands, 2013.

[4] D. Amsallem and C. Farhat. Stabilization of projection-based reduced-order models. Int. J. Numer. Meth. Engng., 91:358–377, 2012.

[5] D. Amsallem, M. Zahr, Y. Choi, and C. Farhat. Design Optimization Using Hyper-Reduced-Order Models. Technical report, Stanford University, 2013.

[6] E. Arian, M. Fahl, and E.W. Sachs. Trust-region proper orthogonal decomposition for flow control. ICASE: Technical Report 2000-25, 2000.

[7] E. Arian, M. Fahl, and E.W. Sachs. Trust-region proper orthogonal decomposition for flow control. Institute for Computer Applications in Science and Engineering, Hampton VA, 2000.

[8] M. Barrault, Y. Maday, N.C. Nguyen, and A.T. Patera. An 'empirical interpolation' method: application to efficient reduced-basis discretization of partial differential equations. Comptes Rendus Mathematique, 339(9):667–672, 2004.

[9] R. Barrett, M. Berry, T. F. Chan, J. Demmel, J. Donato, J. Dongarra, V. Eijkhout, R. Pozo, C. Romine, and H. Van der Vorst. Templates for the Solution of Linear Systems: Building Blocks for Iterative Methods, 2nd Edition. SIAM, Philadelphia, PA, 1994.

[10] M.M. Baumann. Nonlinear Model Order Reduction using POD/DEIM for Optimal Control of Burgersâquation. Master's thesis, Delft University of Technology, Netherlands, 2013.

[11] M. Bergmann and L. Cordier. Drag minimization of the cylinder wake by trust-region proper orthogonal decomposition. Notes on Numerical Fluid Mechanics and Multidisciplinary Design, 95(16):309–324, 2007.

[12] T. Bui-Thanh, K. Willcox, O. Ghattas, and B. van Bloemen Waanders. Goal-oriented, model-constrained optimization for reduction of large-scale systems. J. Comput. Phys., 224(2):880–896, 2007.

[13] Y. Cao, J. Zhu, I.M. Navon, and Z. Luo. A reduced order approach to four-dimensional variational data assimilation using proper orthogonal decomposition. Int. J. Numer. Meth. Fluids., 53(10):1571–1583, 2007.

[14] S. Chaturantabut. Dimension Reduction for Unsteady Nonlinear Partial Differential Equations via Empirical Interpolation Methods. Technical Report TR09-38,CAAM, Rice University, 2008.

[15] S. Chaturantabut and D.C. Sorensen. Nonlinear model reduction via discrete empirical interpolation. SIAM Journal on Scientific Computing, 32(5):2737–2764, 2010.

[16] S. Chaturantabut and D.C. Sorensen. A state space error estimate for POD-DEIM nonlinear model reduction. SIAM Journal on Numerical Analysis, 50(1):46–63, 2012.

[17] X. Chen, S. Akella, and I. M. Navon. A dual weighted trust-region adaptive POD 4D-Var applied to a Finite-Volume shallow-water Equations Model on the sphere. Int. J. Numer. Meth. Fluids, 68:377–402, 2012.

[18] Xiao Chen, I. M. Navon, and F. Fang. A dual weighted trust-region adaptive POD 4D-Var applied to a Finite -Element Shallow water Equations Model. Int. J. Numer. Meth. Fluids, 68:520–541, 2011.

[19] D.N. Daescu and I.M. Navon. Efficiency of a POD-based reduced second order adjoint model in 4-D VAR data assimilation. Int. J. Numer. Meth. Fluids., 53: 985–1004, 2007.

[20] D.N. Daescu and I.M. Navon. A Dual-Weighted Approach to Order Reduction in 4D-Var Data Assimilation. Mon. Wea. Rev., 136(3):1026–1041, 2008.

[21] M. Dihlmann and B. Haasdonk. Certified PDE-constrained parameter optimization using reduced basis surrogate models for evolution problems. Submitted to the Journal of Computational Optimization and Applications, 2013. URL `http://www.agh.ians.uni-stuttgart.de/publications/2013/DH13`.

[22] G. Dimitriu, N. Apreutesei, and R. Stefanescu. Numerical simulations with data assimilation using an adaptive POD procedure. LNCS, 5910:165–172, 2010.

[23] F. Diwoky and S. Volkwein. Nonlinear boundary control for the heat equation utilizing proper orthogonal decomposition. In Karl-Heinz Hoffmann, RonaldH.W. Hoppe, and Volker Schulz, editors, Fast Solution of Discretized Optimization Problems, volume 138 of ISNM International Series of Numerical Mathematics, pages 73–87. Birkhäuser Basel, 2001. ISBN 978-3-0348-9484-5.

[24] J. Du, I.M. Navon, J. Zhu, F. Fang, and A.K. Alekseev. Reduced order modeling based on POD of a parabolized Navier-Stokes equations model II: Trust region POD 4-D VAR Data Assimilation. Computers and Mathematics with Applications, 69 (3):710–730, 2012.

[25] G. Fairweather and I.M. Navon. A linear ADI method for the shallow water equations. Journal of Computational Physics, 37:1–18, 1980.

[26] F. Fang, C.C. Pain, I.M. Navon, M.D. Piggott, G.J. Gorman, P. E. Farrell, P. Allison, and A.J.H. Goddard. A POD reduced order 4D-Var adaptive mesh ocean modelling approach. Int. J. Numer. Meth. Fluids., 60(7):709–732, 2009.

[27] A. Grammeltvedt. A survey of finite difference schemes for the primitive equations for a barotropic fluid. Monthly Weather Review, 97(5):384–404, 1969.

[28] M.A. Grepl and A.T. Patera. A posteriori error bounds for reduced-basis approximations of parametrized parabolic partial differential equations. ESAIM: Mathematical Modelling and Numerical Analysis, 39(01):157–181, 2005.

[29] M. Gubisch and S. Volkwein. Proper Orthogonal Decomposition for Linear-Quadratic Optimal Control. Technical report, University of Konstanz, 2013.

[30] B. Gustafsson. An alternating direction implicit method for solving the shallow water equations. Journal of Computational Physics, 7:239–254, 1971.

[31] M. Hinze and S. Volkwein. Proper orthogonal decomposition surrogate models for nonlinear dynamical systems: Error estimates and suboptimal control. Lecture Notes in Computational Science and Engineering, 45:261–306, 2005.

[32] M. Hinze and S. Volkwein. Error Estimates for Abstract Linear-Quadratic Optimal Control Problems Using Proper Orthogonal Decomposition. Computational Optimization and Applications, 39(3):319–345, 2008.

[33] M. Hinze and S. Volkwein. Error estimates for abstract linear-quadratic optimal control problems using proper orthogonal decomposition. Computational Optimization and Applications, 39:319–345, 2008.

[34] H. Hotelling. Analysis of a complex of statistical variables with principal components. Journal of Educational Psychology, 24:417–441, 1933.

[35] K. Ito and K. Kunisch. Reduced Order Control Based on Approximate Inertial Manifolds. Linear Algebra and its Applications, 415(2-3):531–541, 2006.

[36] K. Ito and K. Kunisch. Reduced-Order Optimal Control Based on Approximate Inertial Manifolds for Nonlinear Dynamical Systems. SIAM Journal on Numerical Analysis, 46(6):2867–2891, 2008.

[37] M. Kahlbacher and S. Volkwein. POD a-Posteriori Error Based Inexact SQP Method for Bilinear Elliptic Optimal Control Problems. Esaim-Mathematical Modelling and Numerical Analysis-Modelisation Mathematique et Analyse Numerique, 46(2):491–511, 2012.

[38] E. Kammann, F. Tröltzsch, and S. Volkwein. A method of a-posteriori error estimation with application to proper orthogonal decomposition. ESAIM: Mathematical Modelling and Numerical Analysis, 47:555–581, 2013.

[39] K. Karhunen. Zur spektraltheorie stochastischer prozesse. Annales Academiae Scientarum Fennicae, 37, 1946.

[40] C. T. Kelley. Iterative Methods for Linear and Nonlinear Equations. Number 16 in Frontiers in Applied Mathematics. SIAM, 1995.

[41] K. Kunisch and S. Volkwein. Control of the Burgers Equation by a Reduced-Order Approach Using Proper Orthogonal Decomposition. Journal of Optimization Theory and Applications, 102(2):345–371, 1999.

[42] K. Kunisch and S. Volkwein. Proper Orthogonal Decomposition for Optimality Systems. Math. Modelling and Num. Analysis, 42:1–23, 2008.

[43] K. Kunisch and S. Volkwein. Optimal snapshot location for computing POD basis functions. ESAIM: Math. Model. Numer. Anal., M2AN 44(3):509–529, 2010.

[44] K. Kunisch and L. Xie. Pod-Based Feedback Control of the Burgers Equation by Solving the Evolutionary HJB Equation. Computers and Mathematics with Applications, 49(7-8):1113–1126, 2005.

[45] K. Kunisch, S. Volkwein, and L. Xie. HJB-POD-Based Feedback Design for the Optimal Control of Evolution Problems. SIAM J. Appl. Dyn. Syst, 3(4):701–722, 2004.

[46] O. Lass and S. Volkwein. Adaptive POD basis computation for parameterized nonlinear systems using optimal snapshot location. Konstanzer Schriften Math., 304:1–27, 2012.

[47] F. Leibfritz and S. Volkwein. Reduced Order Output Feedback Control Design for PDE Systems Using Proper Orthogonal Decomposition and Nonlinear Semidefinite Programming. Linear Algebra and its Applications, 415(2–3):542–575, 2006.

[48] M.M. Loève. Probability Theory. Van Nostrand, Princeton, NJ, 1955.

[49] E.N. Lorenz. Empirical Orthogonal Functions and Statistical Weather Prediction. Technical report, Massachusetts Institute of Technology, Dept. of Meteorology, 1956.

[50] I. M. Navon and R. De Villiers. Gustaf: A Quasi-Newton nonlinear ADI fortran iv program for solving the shallow-water equations with augmented lagrangians. Computers and Geosciences, 12(2):151–173, 1986.

[51] A.T. Patera and G. Rozza. Reduced basis approximation and a posteriori error estimation for parametrized partial differential equations, 2007.

[52] Joanna S. Pelc, Ehouarn Simon, Laurent Bertino, Ghada El Serafy, and Arnold W. Heemink. Application of model reduced 4D-Var to a 1D ecosystem model. Ocean Modelling, 57–58(0):43 –58, 2012. ISSN 1463-5003.

[53] S.S. Ravindran. Adaptive Reduced-Order Controllers for a Thermal Flow System Using Proper Orthogonal Decomposition. J. Sci. Comput., 23:1924–1942, 2002.

[54] G. Rozza, D.B.P. Huynh, and A.T. Patera. Reduced basis approximation and a posteriori error estimation for affinely parametrized elliptic coercive partial differential equations. Archives of Computational Methods in Engineering, 15(3):229–275, 2008.

[55] Y. Saad. Sparsekit: a basic tool kit for sparse matrix computations. Technical Report, Computer Science Department, University of Minnesota, 1994.

[56] Y. Saad. Iterative Methods for Sparse Linear Systems. Society for Industrial and Applied Mathematics, Philadelphia, PA, USA, 2nd edition, 2003.

[57] E. W. Sachs and S. Volkwein. POD-Galerkin Approximations in PDE-Constrained Optimization. GAMM-Mitteilungen, 33(2):194–208, 2010.

[58] D. Sava. Model-Reduced Gradient Based Production Optimization. (M.S) Delft University of Technology, 2012.

[59] D.F. Shanno and K.H. Phua. Remark on algorithm 500 - a variable method subroutine for unconstrained nonlinear minimization. ACM Transactions on Mathematical Software, 6:618–622, 1980.

[60] R. Stefanescu and I.M. Navon. POD/DEIM Nonlinear model order reduction of an ADI implicit shallow water equations model. Journal of Computational Physics, 237:95–114, 2013.

[61] R. Stefanescu, A. Sandu, and I.M. Navon. Comparisons of POD reduced order strategies for the nonlinear 2D Shallow Water Equations Model. Technical Report TR 2, Virginia Polytechnic Institute and State University, February 2014, also submitted to International Journal for Numerical Methods in Fluids.

[62] T. Tonna, K. Urbana, and S. Volkwein. Comparison of the Reduced-Basis and POD a-Posteriori Error Estimators for an Elliptic Linear-Quadratic Optimal Control Problem. Mathematical and Computer Modelling of Dynamical Systems: Methods, Tools and Applications in Engineering and Related Sciences, 17(4):355–369, 2010.

[63] F. Tröltzsch and S. Volkwein. POD a-Posteriori Error Estimates for Linear-Quadratic Optimal Control Problems. Computational Optimization and Applications, 44(1):83–115, 2009.

[64] P.T.M. Vermeulen and A.W. Heemink. Model-reduced variational data assimilation. Mon. Wea. Rev., 134:2888–2899, 2006.

[65] K. Willcox and J. Peraire. Balanced model reduction via the Proper Orthogonal Decomposition. AIAA Journal, pages 2323–2330, 2002.

Appendix

This appendix contains a symbolic representation of the Gustafsson's nonlinear ADI finite difference shallow water equations schemes defined in (18) which allow us to characterize their corresponding discrete tangent linear and adjoint models.

ADI SWE scheme requires two steps to solve for $\boldsymbol{u}^{N+1}, \quad \boldsymbol{v}^{N+1}, \quad \boldsymbol{\phi}^{N+1}$.

First step - get solution at $t_{N+\frac{1}{2}}$

$$\begin{aligned}
D_{-t}\mathbf{u}^{N+\frac{1}{2}} &= -F_{11}(\mathbf{u}^{N+\frac{1}{2}}) - F_{12}(\boldsymbol{\phi}^{N+\frac{1}{2}}) - F_{13}(\mathbf{u}^{N}, \mathbf{v}^{N}) + \mathbf{F} \odot \mathbf{v}^{N}, \\
D_{-t}\mathbf{v}^{N+\frac{1}{2}} &= -F_{21}(\mathbf{u}^{N+\frac{1}{2}}) - F_{22}(\mathbf{v}^{N}) - F_{23}(\boldsymbol{\phi}^{N}) - \mathbf{F} \odot \mathbf{u}^{N+\frac{1}{2}}, \\
D_{-t}\boldsymbol{\phi}^{N+\frac{1}{2}} &= -F_{31}(\mathbf{u}^{N+\frac{1}{2}}, \boldsymbol{\phi}^{N+\frac{1}{2}}) - F_{32}(\mathbf{u}^{N+\frac{1}{2}}, \boldsymbol{\phi}^{N+\frac{1}{2}}) - F_{33}(\mathbf{v}^{N}, \boldsymbol{\phi}^{N}) - F_{34}(\mathbf{v}^{N}, \boldsymbol{\phi}^{N}),
\end{aligned} \tag{23}$$

where $D_{-t}^{N+\frac{1}{2}}\mathbf{w}$ is the backward in time difference operator, $\mathbf{w} = (\mathbf{u}, \mathbf{v}, \boldsymbol{\phi})$, $\odot$ is the component-wise multiplication operator, $\mathbf{F} = [\underbrace{\mathbf{f}, \mathbf{f}, .., \mathbf{f}}_{N_x}]$ stores Coriolis components $\mathbf{f} = [f(y_j)]_{j=1,2,..,N_y}$ while the nonlinear terms $F_{i,j}$ are defined in (21).

Second step - get solution at t_{N+1}

$$\begin{aligned}
D_{-t}\mathbf{u}^{N+1} &= -F_{13}(\mathbf{u}, \mathbf{v}^{N+1}) + \mathbf{F} \odot \mathbf{v}^{N+1} - F_{11}(\mathbf{u}^{N+\frac{1}{2}}) - F_{12}(\boldsymbol{\phi}^{N+\frac{1}{2}}), \\
D_{-t}\mathbf{v}^{N+1} &= -F_{22}(\mathbf{v}^{N+1}) - F_{23}(\boldsymbol{\phi}^{N+1}) - F_{21}(\mathbf{u}^{N+\frac{1}{2}}) - \mathbf{F} \odot \mathbf{u}^{N+\frac{1}{2}}, \\
D_{-t}\boldsymbol{\phi}^{N+1} &= -F_{33}(\mathbf{v}^{N+1}, \boldsymbol{\phi}^{N+1}) - F_{34}(\mathbf{v}^{N+1}, \boldsymbol{\phi}^{N+1}) - F_{31}(\mathbf{u}^{N+\frac{1}{2}}, \boldsymbol{\phi}^{N+\frac{1}{2}}) - F_{32}(\mathbf{u}^{N+\frac{1}{2}}, \boldsymbol{\phi}^{N+\frac{1}{2}}).
\end{aligned} \tag{24}$$

The nonlinear systems of algebraic equations (23) and (24) are solved using quasi-Newton method, thereby we rewrite them in the form

$$\mathbf{g}(\boldsymbol{w}) = 0, \quad \mathbf{g}(\boldsymbol{w}) = \begin{pmatrix} g_1(\boldsymbol{w}) \\ g_2(\boldsymbol{w}) \end{pmatrix},$$

where $\mathbf{g_1}$ and $\mathbf{g_2}$ represent systems (23) and (24). The corresponding iterative Newton steps are:

$$\begin{aligned}
\boldsymbol{w}^{N+\frac{1}{2}} &= \boldsymbol{w}^{N} - J_1^{-1}(\boldsymbol{w}^{N}) g_1(\boldsymbol{w}^{N}), \\
\boldsymbol{w}^{N+1} &= \boldsymbol{w}^{N+\frac{1}{2}} - J_2^{-1}(\boldsymbol{w}^{N+\frac{1}{2}}) g_2(\boldsymbol{w}^{N+\frac{1}{2}}),
\end{aligned} \tag{25}$$

where $J_1, J_2 \in \mathbb{R}^{3n\times 3n}$ denotes the Jacobians

$$J_1 = \frac{\partial g}{\partial \boldsymbol{w}^N}, \qquad J_2 = \frac{\partial g}{\partial \boldsymbol{w}^{N+\frac{1}{2}}}.$$

Then, the corresponding tangent linear model is

$$\begin{cases} J_1(\boldsymbol{w}^N)\boldsymbol{\delta} w^{N+\frac{1}{2}} = J_2(\boldsymbol{w}^N)\boldsymbol{\delta} w^N, \\ J_2(\boldsymbol{w}^{N+\frac{1}{2}})\boldsymbol{\delta} w^{N+1} = J_1(\boldsymbol{w}^{N+\frac{1}{2}})\boldsymbol{\delta} w^{N+\frac{1}{2}}, \end{cases} \tag{26}$$

and $\boldsymbol{\delta} w = (\boldsymbol{\delta} u, \boldsymbol{\delta} v, \boldsymbol{\delta}\phi)$ are the tangent linear unknowns.

The adjoint model is obtained by transposing (26)

First step - get solution at $t_{N+\frac{1}{2}}$

$$\begin{cases} \left[J_2(\boldsymbol{w}^{N+\frac{1}{2}})\right]^T \boldsymbol{z}^{N+1} = \boldsymbol{\lambda}^{N+1}, \\ \boldsymbol{\lambda}^{N+\frac{1}{2}} = \left[J_1(\boldsymbol{w}^{N+\frac{1}{2}})\right]^T \boldsymbol{z}^{N+1}. \end{cases} \tag{27}$$

Second step - get solution at t_N

$$\begin{cases} \left[J_1(\boldsymbol{w}^{N})\right]^T \boldsymbol{z}^{N+\frac{1}{2}} = \boldsymbol{\lambda}^{N+\frac{1}{2}}, \\ \boldsymbol{\lambda}^{N} = \left[J_2(\boldsymbol{w}^{N})\right]^T \boldsymbol{z}^{N+\frac{1}{2}}, \end{cases} \tag{28}$$

where $\boldsymbol{\lambda} = (\boldsymbol{\lambda}_u, \boldsymbol{\lambda}_v, \boldsymbol{\lambda}_\phi)$ are the adjoint unknowns and $\boldsymbol{z}$ is an intermediary variable. By $\left[J_1(\boldsymbol{w}^N)\right]^T$ we denote the transpose of Jacobian $J_1(\boldsymbol{w}^N)$.